Manuscript Details

Manuscript number	JPHOTOCHEM_2019_322_R1
Title	Black carbon-doped TiO2 films: synthesis, characterization and photocatalysis
Article type	Full length article

Abstract

Black colour TiO2 films were synthesized on amorphous fused silica substrates by DC magnetron sputtering technique with carbon powders placed at the working magnetron surface. Comprehensive sample analysis by X-ray diffraction, energy dispersive X-ray spectroscopy and X-ray photoelectron spectroscopy showed that the rutile/anatase heterostructure TiO2 films were successfully formed. Moreover, observation of O-Ti-C bonds confirmed that TiO2 phase was doped by carbon additives. Scanning electron microscopy, atomic force microscopy and X-ray diffraction were used to identify the effect of deposition time and TiO2 film thickness on the surface morphology, roughness and crystallite size. Results of electron spin resonance showed that oxygen vacancies were generated on the surface with trapped unpaired electrons. Optical analysis by UV-Vis light spectrophotometer showed that TiO2 films with carbon additives improve its capability to absorb visible light. Accordingly, methylene blue bleaching experiments under UV-A and visible light irradiation showed that black colour TiO2 films are capable to decompose methylene blue solution at both UV-A and visible light irradiation.

Keywords	Photocatalysis; black TiO2; carbon-doped TiO2; magnetron sputtering; band gap; visible light
Manuscript region of origin	Europe

Corresponding Author	Sarunas Varnagiris
Corresponding Author's Institution	Lithuanian energy institute
Order of Authors	Sarunas Varnagiris, Arturs Medvids, Martynas Lelis, Darius Milcius, Andris Antuzevics
Suggested reviewers	Suresh Pillai, Marina Ratova, Reza Dariani

Submission Files Included in this PDF

File Name [File Type]

Cover_letter-resubmission.docx [Cover Letter]

Response to the reviewers.docx [Response to Reviewers]

Highlights.docx [Highlights]

Graphical abstract.tiff [Graphical Abstract]

Manuscript.docx [Manuscript File]

Fig 1.tiff [Figure]

Fig 2.tif [Figure]

Fig 3.tif [Figure]

Fig 4.tiff [Figure]

Fig 5.tiff [Figure]

Fig 6.tiff [Figure]

Fig 7.tif [Figure]

Fig 8.tiff [Figure]

Fig 9.tiff [Figure]

To view all the submission files, including those not included in the PDF, click on the manuscript title on your EVISE Homepage, then click 'Download zip file'.

Revision and resubmission of manuscript JPHOTOCHEM_2019_322

14 June, 2019

Dear Editor Prof. Steve Meech,

Please consider our revised manuscript “Black carbon-doped TiO2 films: synthesis, characterization and photocatalysis” to the Journal of Photochemistry and Photobiology A: Chemistry (Ref: JPHOTOCHEM_2019_322).

We highly appreciate all reviewer comments, which were very constructive and helpful. We corrected our paper according to reviewers’ comments. More specifically additional experiments of EDS elemental mapping and electron spin resonance were performed. Photocatalytic degradation mechanism of black carbon-doped TiO_2 was provided towards the degradation of MB. English language was polished. The introduction part was extended with additional paragraphs: i) the fundamental works in the use of the magnetron sputtering in general; ii) recent progress in the deposition of C-doped TiO_2 coatings; iii) advantage of the used methodology; according to reviewer comments. Also, experimental details, choice of the MB for the photocatalytic activity measurements, additional explanations of XPS and XRD measurements were added to the manuscript. These changes have clearly improved our manuscript.

We have also included a point-by-point response to the reviewer’s comments. Changes to the text in the manuscript are highlighted.

Thank you for consideration of our revised manuscript.

Thank you very much for Your consideration.

Dr. Sarunas Varnagiris
Lithuanian Energy Institute
Breslaujos str. 3, Kaunas, Lithuania
Tel.: +37066243136
E-mail: sarunas.varnagiris@lei.lt

Response to the reviewers

14 June, 2019

Dear Reviewers,

First of all, we would like to thank you for constructive comments which help to improve the quality of this manuscript. The response to comments could be found below.

Reviewer 1

An in-situ synthetic method was introduced to prepare black colour rutile/anatase heterostructure TiO2 films via DC magnetron sputtering technique. The new photocatalyst is characterized including SEM and AFM. Crystal structure, binding energy and absorption spectrum were characterized by EDX, and XPS. Additionally, this manuscript was well presented with some experimental data. However, the reviewer would suggest the authors to consider the following points, which might be taken for a major revision:

1. STEM Mapping should be provided to obtain the elements distribution, especially for carbon element.

Answer: Elemental mapping was performed to obtain Ti, O and C elements distribution. Results showed that elements are distributed relatively uniform in whole TiO_2 film area. Similar tendencies persist in all TiO_2 films.

Text added to the manuscript:

EDS mapping was performed in order to evaluate carbon distribution in TiO_2 films. Fig. 1. shows EDS mapping views of Ti, O, C elements. Fig. 1. shows EDS mapping views of Ti, O, C elements. It is evident that for all samples carbon, titanium and oxygen are uniformly distributed over whole analyzed area of TiO_2 films.

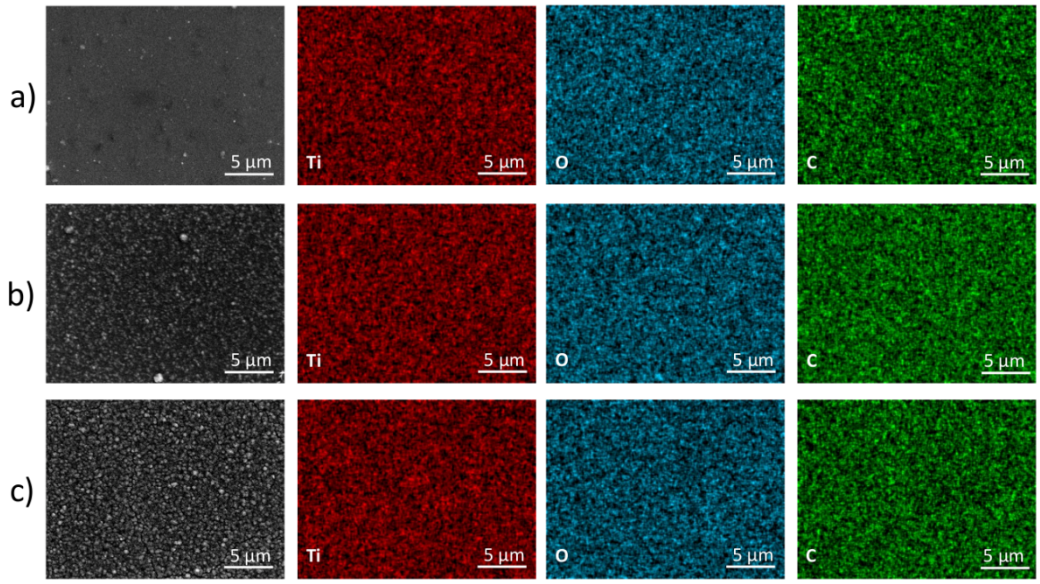

Fig. 1. EDS mapping views of Ti, O, C elements after deposition time of : a) 60 min, b) 120 min, c) 180 min.

(see manuscript, page 9-10)

2. The optical and electrochemical properties of black carbon-doped TiO2 need to be measured by photoluminescence (PL) spectroscopy, and the electron spin resonance (ESR).

Answer: The electrochemical properties of black carbon-doped TiO_2 was measured by electron spin resonance (ESR). Results showed that oxygen vacancies were generated on the surface with trapped unpaired electrons. Unfortunately, measurements of photoluminescence (PL) spectroscopy wasn't prepared due to equipment failure which wasn't fixed by the time.

Text added to the manuscript:

(experimental part)

The electron paramagnetic resonance (EPR) spectra of black colour carbon doped TiO2 were obtained using Bruker ELEXSYS-II E500 CW-EPR spectrometer operated at 100 kHz modulation frequency, room temperature X-band (≈ 9.36 GHz) and 2 G modulation amplitude. Samples were cut and placed in identical quartz EPR tubes ensuring equal positioning of the tubes within the resonator. EPR spectra have been averaged across 30 scans and normalized to the sample mass.

(see manuscript, page 9-10)

(Results)

It is known that atoms or molecules with unpaired electrons have a significant influence in photocatalysis, which can be quantitatively and qualitatively evaluated by ESR [55,56]. Measurements of ESR were performed at room temperature to characterize the unpaired electrons or paramagnetic centers. ESR spectra of the investigated films are shown in Fig. 7. The results showed that very strong ESR signal at g = 2.003 ± 0.001 was observed by TiO_2 film after 180 min deposition. This could be attributed to the unpaired electron trapped on surface oxygen vacancies [57,58]. Significant weaker signals at about g = 2.001 ± 0.001 were observed for TiO_2 films after 60 min and 120 min deposition respectively. Such significant decrease of ESR spectra intensity implies the reduction of the Ti^{3+} spins. The ESR results demonstrate that longer deposition time may contribute to the generation of oxygen vacancies while TiO_2 is doped by carbon. Similar results were observed by other authors where carbon or other dopants invoke generation of oxygen vacancies in TiO_2 [59–62].

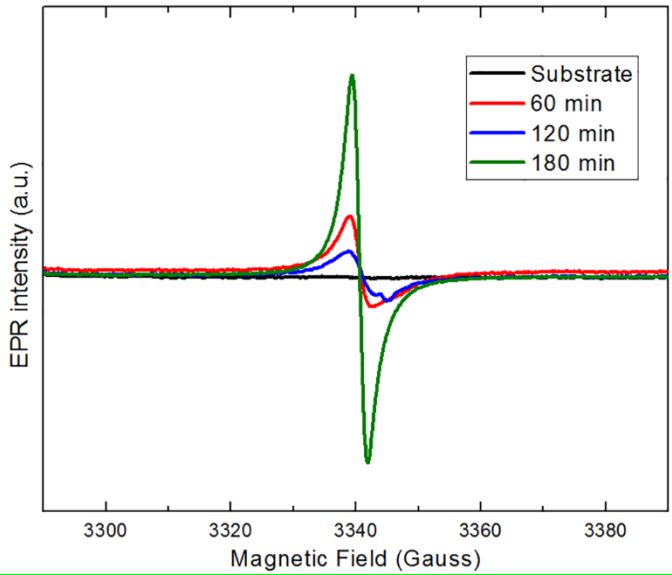

Fig. 2. ESR spectra views of TiO_2 films at room temperature

(see manuscript, page 15-16)

3. Photocatalytic degradation mechanism of black carbon-doped TiO2 should be provided towards

the degradation of MB.

Answer: Photocatalytic properties of carbon-doped TiO2 films were tested by investigating bleaching of the MB in aqueous solution under UV-A and visible light irradiation. Irradiation intensities at the surface of the sample were 12 mW/cm^2 and 24.5 mW/cm^2 for UV-A and visible light respectively. The natural decay rate of methylene blue without the photocatalyst under UV-A and visible light sources was measured for reference purposes. The degradation rate of MB solution in contact with photocatalyst but without light irradiation was also evaluated. Both cases showed negligible degradation of MB solution. Results of MB bleaching experiment showed that all deposited carbon-doped TiO_2 films exhibit photocatalytic decomposition properties. The highest decomposition ratio was observed by using carbon-doped TiO_2 film after 180 min deposition time (k values 3.18×10-3 min-1 with UV-A and 1.14×10-3 min-1 with visible 455 nm light irradiation) while the lowest decomposition ratio was observed by carbon-doped TiO2 films after 60 min deposition time (k values 1.03×10-3 min-1 with UV-A and 0.67×10-3 min-1 with visible 455 nm light irradiation). More results and discussion of photocatalytic degradation mechanism of black carbon-doped TiO2 towards the degradation of MB are presented in **17-19 pages of manuscript**.

4. English need to be polished.

The English grammar and structure of sentences were revised and corrected.

Reviewer 2

The authors here present a study on C-doped TiO2 films prepared by magnetron sputtering to improve visible light photocatalytic activity. While the subject of the paper is interesting and appropriate for the readership of the journal, the organisation of the paper and the data presented leave some questions that should be answered by authors to make the work publishable.

In particular, I suggest the authors to respond to the comments below:

1. The reference list should be extended to reflect the state-of-art in the field. In particular, the authors are advised to reference the fundamental works in the use of the magnetron sputtering in general, and the application of it to the production of TiO2 works in particular. I would suggest the following papers should be included:

P.J. Kelly, R.D. Arnell, Magnetron sputtering: a review of recent developments and applications, Vacuum 56(3) (2000) 159-172.

P.J. Kelly, G.T. West, M. Ratova, L. Fisher, S. Ostovarpour, J. Verran, Structural Formation and Photocatalytic Activity of Magnetron Sputtered Titania and Doped-Titania Coatings, Molecules 19(10) (2014) 16327-16348.

J. Šícha, D. Heřman, J. Musil, Z. Strýhal, J. Pavlík, Surface Morphology of Magnetron Sputtered TiO2 Films, Plasma Processes and Polymers 4(S1) (2007) S345-S349.

Also, the recent progress in the deposition of C-doped TiO2 coatings has not been reviewed. Advantage of the used methodology should be highlighted, as well as comparison of the authors' findings with the earlier works in the subject, such as:

M. Ratova, R. Klaysri, P. Praserthdam, P.J. Kelly, Visible light active photocatalytic C-doped titanium dioxide films deposited via reactive pulsed DC magnetron co-sputtering: Properties and photocatalytic activity, Vacuum 149 (2018) 214-224.

D. Xie, F. Wen, W. Yang, X. Li, Y. Leng, G. Wan, H. Sun, N. Huang, Carbon-Doped Titanium Oxide Films by DC Reactive Magnetron Sputtering Using CO2 and O2 as Reactive Gas, Acta Metallurgica Sinica (English Letters) 27(2) (2014) 239-244.

F. Wen, C. Zhang, D. Xie, H. Sun, Y.X. Leng, Research of composition and photocatalytic property of carbon-doped Ti-O films prepared by R-MS using CO2 gas resource, Nuclear Instruments & Methods in Physics Research Section B-Beam Interactions with Materials and Atoms 307 (2013) 381-384.

R. Klaysri, M. Ratova, P. Praserthdam, P. Kelly, Deposition of Visible Light-Active C-Doped Titania

Films via Magnetron Sputtering Using CO2 as a Source of Carbon, Nanomaterials 7(5) (2017) 113.

Answer: Thank you for your comments and suggestions how to improve a review part. The suggested areas (the fundamental works in the use of the magnetron sputtering, the application of it to the production of TiO2, the recent progress in the deposition of C-doped TiO2 coatings) were reviewed based on your recommended and other papers. The advantages of used methodology were highlighted and comprised with the earlier works. All suggested articles were cited in this work.
Text added to the manuscript:
The present report describes the experimental investigation of the photocatalytically active black colour TiO2 formation by using a magnetron sputtering technique. Magnetron sputtering is a widely used technique for the production of high quality coatings due to its scalability, versatility, uniformity and repeatability [41]. J. Sicha et al. showed possibility to control deposited TiO2 film structure and surface morphology by changing deposition rate, partial oxygen pressure or mode of sputtering [42]. Moreover, P. J. Kelly et al. demonstrated that the choice of MS deposition technique as well as dopant element has significant influence on structural formation and photocatalytic activity of deposited coatings [43]. One of the most suitable dopant for improvement of TiO2 photocatalytic activity is carbon.
Various methods can be used to prepare magnetron sputtered C-doped TiO2 coatings. R. Klaysri et al. used pulsed direct current magnetron sputtering for the deposition of carbon-doped titania coatings with CO2 gas as the source of carbon. The promising photocatalytic activity was observed while deposited C-doped TiO2 films could decompose methylene blue dye under visible light irradiation [44]. Similar magnetron sputtering technique with CO2 gas as carbon source was applied by other authors [45,46]. Two magnetron co-sputtering technique via reactive pulsed DC power source was successfully applied for photocatalytical active C-doped TiO2 film formation [47]. However all these methods require appliance of annealing or BIAS voltage.
In this study novel magnetron sputtering technique was used to deposit photocatalytical active black colour C-doped TiO2 films. The deposition was performed using magnetron system with Ti cathode. Carbon powders were placed on the top of cathode. This method requires only one magnetron during deposition while polycrystalline anatase/rutile phase could be performed at room temperature. The analysis of the results is focussed on the surface characterisation, chemical bonds, light absorption and decomposition of methylene blue solution under UV and visible light irradiation. ***(see manuscript, page 4-5)***

2. Experimental details are incomplete. Thus, for the deposition process, the details of the magnetron are missing, making the deposition process unsuitable to be reproduced, if required. In particular, information on geometrical size of the magnetron, balanced / unbalanced, substrate - target distance, presence of rotation, size of carbon-covered area should be given.
Thank you for this comment. The experimental part was supplemented with the missing information ***(see manuscript, page 5-6)***.
Text added to the manuscript:
Carbon-doped TiO2 films were deposited using unbalanced magnetron sputtering technique with Ti cathode (95 mm diameter, 99.99 % purity). Carbon powder (99.5 % purity) was used for the in-situ TiO2 film doping. For each experiment 2 g of carbon powder was divided into four parts and placed on Ti cathode as shown in Fig. 1. The size of carbon-covered area on Ti cathode was approximately 1.2 cm2 for each carbon part. The selected amount of carbon powder was predetermined experimentally finding optimal conditions for the formation of carbon-doped TiO2 films. Each deposition process was started at room temperature and no auxiliary heat treatment was used

during or after deposition. During the deposition high purity (99.999 %) oxygen gas was kept at a constant 1.3 pressure. Films were deposited on flat (Ra < 1 nm) fused silica substrates (total size 10×20 mm, covered part 10×15 mm) using DC sputtering power of 675 W (current – 1.5 A, voltage 450 V). Prior to magnetron sputtering fused silica substrates were washed in isopropyl alcohol in an ultrasonic bath and then dried out under dry air flow. The distance between the sample and Ti cathode was fixed at 5 cm. As samples were placed directly above the magnetron, sample size was significantly smaller than the cathode diameter and there were no indications of films inhomogeneity. Therefore, deposition of TiO2 films was performed without any additional rotation of the substrate. During experiments magnetron sputtering was performed for 60, 120 and 180 min.

For the photocatalytic test, the irradiance patterns of the light sources used would be advantageous for the paper. Also, the choice of the MB for the photocatalytic activity measurements should be explained with the great care; as dyes can be easily photosensitized with the visible light and therefore not necessarily representative of the true values of the photocatalytic activity. Authors should comment on this fact when explaining the choice of the model pollutant.

Answer: The irradiance patterns of the light sources could be easily found in manufacturer web page by using lamps codes (Thorlabs M365PL1-C5 lamp and Thorlabs M455L3-C5 lamp) which were added to the manuscript. The choice of the MB for the photocatalytic activity measurements was explained in 2.3 Testing of photocatalytic properties part.

Text added to the manuscript:

Methylene blue is cationic dye with molecular formula C16H18ClN3S. Photocatalytic decomposition of methylene blue can be expressed by following equation [47]:

$$C_{16}H_{18}ClN_3S + 25.5O_2 \xrightarrow[TiO2,\ h\nu \geq BG]{} HCl + H_2SO_4 + 3HNO_3 + 16CO_2 + 6H_2O \quad (1)$$

Changes in monitoring peak height (strongest absorption peak at ca. 665 nm) were used for monitoring the concentration of MB solution. It is known that MB could be photosensitized with the light irradiation and as a consequence perverts the true values of photocatalytic activity. In order to avoid such experimental inaccuracy, the influence of UV and visible light irradiation on MB degradation was evaluated prior to photocatalysis experiment. ***(see manuscript, page 7-8)***

3. It is unclear why in some sections authors compare the C-doped films with the pure TiO2, while in the others not. It would be useful to know how the presence of C influenced all properties of the films, compared to undoped TiO2, in particular comparison should be drawn in terms of phase composition, photocatalytic performance, surface roughness.

Answer: We totally agree with reviewer comment that it would be useful to know how the presence of C influenced all properties of the films, compared to undoped TiO2. It was decided to perform additional experiments in order to compare pure TiO2 with black colour TiO2 films. However, this work covers various analysis methods (SEM, AFM, XRD, XPS, VIS-IR absorption, photocatalysis). Additionally, according to other reviewer comments, EDS elemental mapping, photoluminescence spectroscopy and electron spin resonance measurements were performed. Thus, it was decided to prepare separate article based on comparison of pure TiO2 with black colour TiO2 films. As a consequence, all the information of pure white colour TiO2 (which was shown in Fig. 6) was removed.

4. Were the samples post-deposition heat-treated? If not, what was the deposition temperature?

Answer: Each deposition process was started at room temperature and no auxiliary heat treatment was used during or after deposition. The temperature was monitored at the surface of TiO2 film during deposition process and it wasn't higher that 70^{o} C degree. ***(see manuscript, page 6)***

5. How the chemical composition of samples was calculated with the XPS? Were samples sputter pre-cleaned? Was the elemental carbon peak (C-C) included to the calculation? If so, this carbon is adventitious and can not be considered as doping result.

Answer: Prior to XPS measurements the surface of TiO2 samples was pre-cleaned using Ar^{+} ions.

This led to avoid adventitious carbon during the analysis. Nevertheless, strong carbon peak was observed even after pre-cleaning process ***(see manuscript, page 13-14)***. Thus, C-C peak cannot be considered as adventitious carbon. C1s peak was fitted with four different components based on XPS database, Y. Park et al. and X. Wu et al. works [6–8]. The amount of doped carbon (O-Ti-C bond) was evaluated after fitting process of C1s peak, while software gives an information about different components covered part of total C1s peak in percent. The Multipak software was used for XPS analysis.

6. How the XRD crystallite sizes were calculated? This information should be added to the text.

Answer: The crystallite sizes were evaluated by Topas software with Lorentzian convolution. ***(see manuscript, page 7)***

Highlights

- Black colour TiO_2 films were deposited by magnetron sputtering.
- Chemical bond analysis confirmed that TiO2 phase was doped by carbon.
- Formation of carbon-doped TiO_2 invokes the reduction of band gap.
- TiO_2 films exhibit photocatalytic activity under UV-A and visible light irradiation.

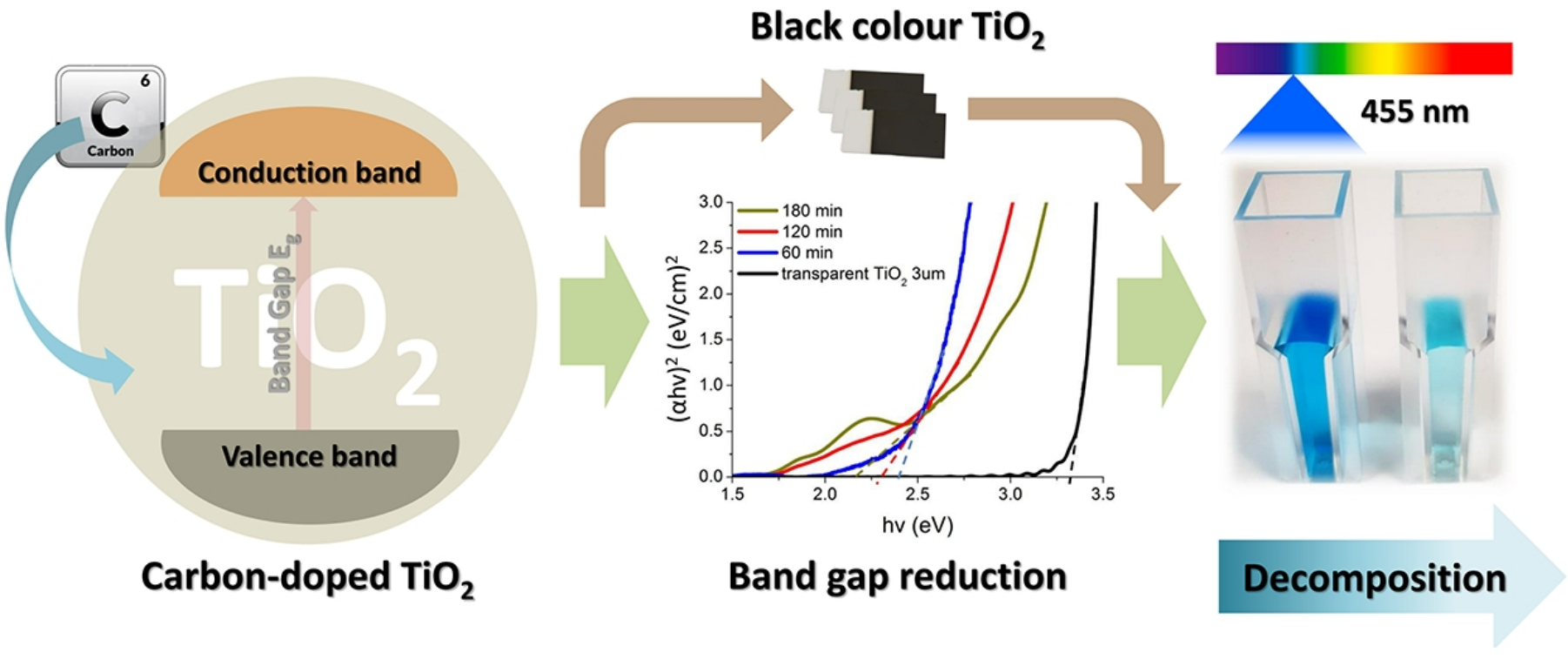
Black colour TiO_2
6
C
Carbon
Conduction band
Band Gap E_g
TiO_2
Valence band
Carbon-doped TiO_2
180 min
120 min
60 min
transparent TiO_2 3um
$(\alpha hv)^2$ (eV/cm)^2
hv (eV)
Band gap reduction
455 nm
Decomposition

Black carbon-doped TiO_2 films: synthesis, characterization and photocatalysis

Sarunas Varnagiris[1*], Arturs Medvids[2], Martynas Lelis[1], Darius Milcius[1], Andris Antuzevics[3]

[1] Lithuanian Energy Institute, 3 Breslaujos Str., LT-4 4403 Kaunas, Lithuania

[2] Technical Physics Institute, Riga Technical University, 3/7 Paula Valdena Str., LV-1048 Riga, Latvia

[3] Institute of Solid State Physics, University of Latvia, 8 Kengaraga Str., LV-1063 Riga, Latvia

* Corresponding author

E-Mail address: sarunas.varnagiris@lei.lt

Graphical abstract

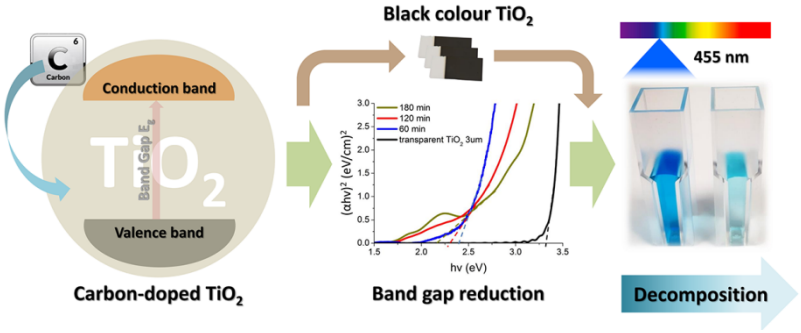

Highlights

- Black colour TiO_2 films were deposited by magnetron sputtering.
- Chemical bond analysis confirmed that TiO2 phase was doped by carbon.
- Formation of carbon-doped TiO_2 invokes the reduction of band gap.
- TiO_2 films exhibit photocatalytic activity under UV-A and visible light irradiation.

Abstract

Black colour TiO_2 films were synthesized on amorphous fused silica substrates by DC magnetron sputtering technique with carbon powders placed at the working magnetron surface. Comprehensive sample analysis by X-ray diffraction, energy dispersive X-ray spectroscopy and X-ray photoelectron spectroscopy showed that the rutile/anatase heterostructure TiO_2 films were successfully formed. Moreover, observation of O-Ti-C bonds confirmed that TiO_2 phase was doped by carbon additives. Scanning electron microscopy, atomic force microscopy and X-ray diffraction were used to identify the effect of deposition time and TiO_2 film thickness on the surface morphology, roughness and crystallite size. Results of electron spin resonance showed that oxygen vacancies were generated on the surface with trapped unpaired electrons. Optical analysis by UV-Vis light spectrophotometer showed that TiO_2 films with carbon additives improve its capability to absorb visible light. Accordingly, methylene blue bleaching experiments under UV-A and visible light irradiation showed that black colour TiO_2 films are capable to decompose methylene blue solution at both UV-A and visible light irradiation.

Keywords: Photocatalysis, black TiO_2, carbon-doped TiO_2, magnetron sputtering, band gap, visible light

1. Introduction

Energy depletion and environmental pollution related problems have become one of the most important areas across the globe in recent decades. Moreover, pollution of air and water become more noticeable due to various human activities. In many cases, effluent water is contaminated with organic dyes that are hardly bio-degradable [1,2]. Although a great consideration is directed to solve these problems, conventional treatment techniques have not been very successful in the purification process [3]. Advanced Oxidation Processes (AOPs) include a more important role in

achieving the degradation of harmful pollutants. AOPs are light-induced processes which are based on the treatment of polluting compounds by making use of hydroxyl radicals (•OH) [4]. During the AOP the radical decomposes toxic organic chemicals by means of its strong oxidizing ability [5,6]. There are four different methods in AOPs to generate hydroxyl radicals and treat wastewater including ozone treatment, electrochemical processes, direct decomposition of water and photocatalysis [7]. Among other AOPs, photocatalysis has received huge attention as one of the most promising environmental purification process [8,9].

The photocatalysis process involves a semiconductor which is activated under light irradiation. During the process, an electron is excited and transferred from the valence band to conduction band. In order to excite an electron, the photocatalyst should absorb photon whose energy is equal or higher to its band gap energy level. This process creates an electron-hole pair which reacts with oxygen molecules, water molecules or hydroxyl groups and generates highly reactive oxygen species (ROS). These ROS react with organic components or pollutants and decompose them during oxidation process [10,11].

Among all the photocatalysts, titanium dioxide (TiO_2) is recognized as a leading photocatalyst for environment purification due to its strong oxidizing power under ultraviolet irradiation, high chemical stability, low cost and other properties. On the other hand, wide band gap (e. g. 3.2 eV for TiO_2 anatase phase) for pure TiO_2 limit its application. Only UV part of solar light spectrum could initiate excitation of electrons and as a consequence electron jumps from a valence band to the conduction band in pristine TiO_2. Moreover, UV radiation contributes only 5 % of the total solar radiation energy at earth surface. Therefore, most of the solar energy is wasted [12–14].

In order to enhance TiO_2 applications in photocatalysis, it is necessary to extend its absorption edge to the visible light region of the solar spectrum as well as to reduce the recombination of the

electron-hole pairs. Various techniques such as doping with metal/non-metal elements [15], control of morphology, usage of different substrates/supports or shapes of TiO_2 [3], reduction of oxygen amount in TiO_2 phases [16], etc. were tried for the formation of TiO_2 with the significant photocatalytic activity under visible light irradiation. Moreover, in order to harvest sunlight more effectively, yellow [17,18], red [19,20], blue [21,22], grey [23,24] and brown TiO_2 [25,26] was also produced. However there are still a lot of issues (secondary impurities, limited or even zero IR region absorption, etc.) which reduce the photocatalytic activity [27]. On the other hand, a lot of researchers showed that black colour TiO_2 demonstrates promising features of wide optical absorption as well as possibility to decompose various pollutants under visible light irradiation [28–31].

Up to now various techniques were used for the synthesis of black TiO_2 nanomaterial including high/low pressure hydrogen treatment [32,33], hydrogen-argon treatment [34,35], hydrogen-nitrogen treatment [36,37], plasma treatment [38,39], metal reduction [40,41], solvothermal synthesis [42], electrochemical reduction-anodization [43] and others. Nevertheless, hydrogenation is the most employed method for synthesizing black TiO_2. However new methods for black TiO_2 synthesis are also required [27].

The present report describes the experimental investigation of the photocatalytically active black colour TiO_2 formation by using a magnetron sputtering technique. Magnetron sputtering is a widely used technique for the production of high quality coatings due to its scalability, versatility, uniformity and repeatability [44]. J. Sicha et al. showed possibility to control structure and surface morphology of deposited TiO_2 films by changing deposition rate, partial oxygen pressure and/or mode of sputtering [45]. Moreover, P. J. Kelly et al. demonstrated that the choice of MS deposition technique as well as dopant element has significant influence on structural formation and

photocatalytic activity of deposited coatings [46]. One of the most suitable dopants for improvement of TiO_2 photocatalytic activity is carbon [47–50].

Various methods can be used to form magnetron sputtered carbon-doped TiO_2 films. R. Klaysri et al. used pulsed direct current magnetron sputtering for the deposition of carbon-doped titania coatings with CO_2 gas as the source of carbon. The promising photocatalytic activity was observed while deposited carbon-doped TiO_2 films could decompose methylene blue dye under visible light irradiation [47]. Similar magnetron sputtering technique with CO_2 gas as carbon source was applied by other authors [48,49]. Two magnetron co-sputtering technique via reactive pulsed DC power source was successfully applied for photocatalytical active carbon-doped TiO_2 film formation [50]. However, all these methods require appliance of annealing or BIAS voltage.

In this study an alternative magnetron sputtering approach was used. Photocatalytic active black colour carbon-doped TiO_2 films were deposited in oxygen atmosphere using single magnetron with Ti cathode. Carbon powders were placed on the top of the cathode. This method required only one magnetron during deposition while polycrystalline anatase/rutile phase could be performed at room temperature. The analysis of the results is focused on the surface characterization, chemical bonds, light absorption and photocatalytic activity by measuring decomposition of methylene blue solution under UV and visible light irradiation.

2. Experimental

2.1 Carbon-doped TiO_2 films deposition

Carbon-doped TiO_2 films were deposited using unbalanced magnetron sputtering technique with Ti cathode (95 mm diameter, 99.99 % purity). Carbon powder (99.5 % purity) was used for the in-situ TiO_2 film doping. For each experiment 2 g of carbon powder was divided into four parts and

placed on Ti cathode as shown in Fig. 1. The size of carbon-covered area on Ti cathode was approximately 1.2 cm^2 for each carbon part. The selected amount of carbon powder was predetermined experimentally finding optimal conditions for the formation of carbon-doped TiO_2 films. Each deposition process was started at room temperature and no auxiliary heat treatment was used during or after deposition. During the deposition high purity (99.999 %) oxygen gas was kept at a constant 1.3 pressure. Films were deposited on flat (Ra < 1 nm) fused silica substrates (total size 10×20 mm, covered part 10×15 mm) using DC sputtering power of 675 W (current – 1.5 A, voltage 450 V). Prior to magnetron sputtering fused silica substrates were washed in isopropyl alcohol in an ultrasonic bath and then dried out under dry air flow. The distance between the sample and Ti cathode was fixed at 5 cm. As samples were placed directly above the magnetron, sample size was significantly smaller than the cathode diameter and there were no indications of films inhomogeneity. Therefore, deposition of TiO_2 films was performed without any additional rotation of the substrate. During experiments magnetron sputtering was performed for 60, 120 and 180 min.

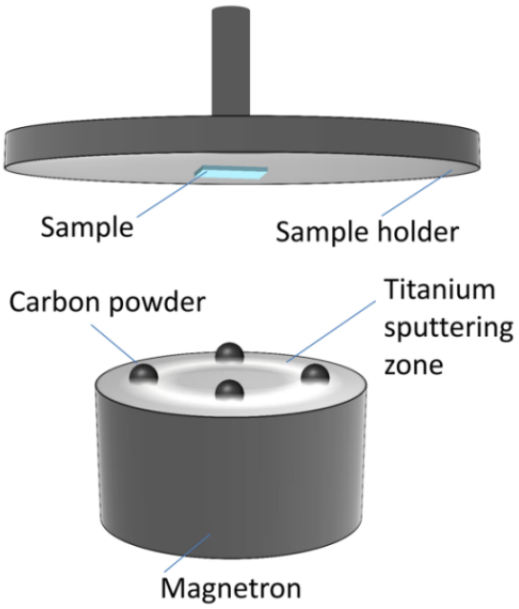

Fig. 1. Scheme of experimental set-up during carbon-doped TiO_2 formation.

2.2 Characterization

As-deposited carbon-doped TiO_2 films were analyzed using stylus profiler (Ambios XP-200) for thickness measurement. Surface morphology measurement was performed with a scanning electron microscope (SEM, Hitachi S-3400N) using a secondary electron detector. Energy dispersive X-ray spectroscopy (EDS, Bruker Quad 5040) was used for the analysis of elemental composition and elemental mapping of TiO2 films. Phase structure of the deposited films was identified by X-Ray diffractometer (XRD, Bruker D8) operating with Cu Kα radiation. The crystallite sizes were evaluated by Topas software with Lorentzian convolution. Surface roughness was evaluated by an atomic force microscope (AFM, Microtestmachines NT-206). Chemical state of the deposited TiO_2 films was analyzed with X-ray photoelectron spectrometer (XPS, PHI Versaprobe 5000) using monochromated 1486.6 eV Al radiation, 25 W beam power, 100 µm beam size and 45° measurement angle. Sample charging was compensated using dual neutralization system consisting of low energy electron beam and ion beam. Prior to XPS measurements the surface of TiO2 samples was pre-cleaned using Ar^+ ions. The electron paramagnetic resonance (EPR) spectra of black colour carbon doped TiO2 were obtained using Bruker ELEXSYS-II E500 CW-EPR spectrometer operated at 100 kHz modulation frequency, room temperature X-band (≈ 9.36 GHz) and 2 G modulation amplitude. Samples were cut and placed in identical quartz EPR tubes ensuring equal positioning of the tubes within the resonator. EPR spectra have been averaged across 30 scans and normalized to the sample mass.

2.3 Testing of photocatalytic properties

Photocatalytic properties of carbon-doped TiO_2 films were tested by investigating bleaching of the aqueous Methylene Blue (MB; Reachem Slovakia s.r.o.) solution under UV-A (Thorlabs M365PL1-C5 lamp; nominal wavelength 365 nm, beam diameter 43 mm) and visible light (Thorlabs M455L3-

C5 lamp; nominal wavelength 455 nm, beam diameter 43 mm) irradiation. Methylene blue is cationic dye with molecular formula $C_{16}H_{18}ClN_3S$. Photocatalytic decomposition of methylene blue can be expressed by the following equation [50]:

$$C_{16}H_{18}ClN_3S + 25.5O_2 \underset{TiO2,\, hv \geq BG}{\Rightarrow} HCl + H_2SO_4 + 3HNO_3 + 16CO_2 + 6H_2O \quad (1)$$

Changes of the strongest peak intensity (absorption peak at ca. 665 nm) were used for the determination of the MB solution concentration. It is known that MB could be photosensitized with the light irradiation and as a consequence perverts the true values of photocatalytic activity [51]. Therefore, in order to estimate such experimental inaccuracy, the influence of UV and visible light irradiation on MB degradation was evaluated separately prior to the photocatalysis experiments.

For the photocatalysis experiments samples were placed into 30 mm diameter Petri dish. Before the measurements with the selected irradiation samples were kept in the dark for 24 hours. The UV-A and visible light exposure experiments were started straight after 3 ml of 20 mg/L concentration aqueous MB solution was syringed above the samples and top of the petri dish was covered by fused silica disc to minimize evaporation of MB solution. Irradiation intensities at the surface of the sample were 12 mW/cm^2 and 24.5 mW/cm^2 for UV-A and visible light respectively (measured using Thorlabs PM16-401 Power meter).

UV-VIS spectrophotometer (Jasco V-650) was used for the tracking of MB concentration changes. All measurements were repeated regularly at 30 minutes intervals with 1.5 ml volume. MB solution was syringed back to the petri dish with the sample immediately after the spectroscopic analysis (approximately 2 minutes).

3. Results and Discussion

EDS elemental analysis confirmed that deposited films consisted only from titanium, oxygen and carbon. There were no additional impurities or traces element observed. It is important to mention that the amount of doped carbon increased with the longer deposition time (see table 1.). Carbon concentrations were 1.65 at. %, 2.23 at. % and 3.74 at. % for TiO_2 films deposited for 60 min, 120 min and 180 min respectively.

SEM surface views of carbon-doped TiO_2 films after different deposition times are shown in Fig. 2. It can be seen that in all cases carbon-doped TiO_2 films had rough surface with irregular shaped features which consist of different size grains (approximate grains sizes were 50-150 nm for 60 min, 300-400 nm for 120 min and 400-500 nm for 180 min deposited carbon-doped TiO_2 films respectively). Moreover, it was observed that clusters size increased with the larger film thickness. Measured film thickness was approximately 1100 nm for 60 min deposited sample, 2250 nm for 120 min deposited sample and 3325 nm for 180 min deposited sample.

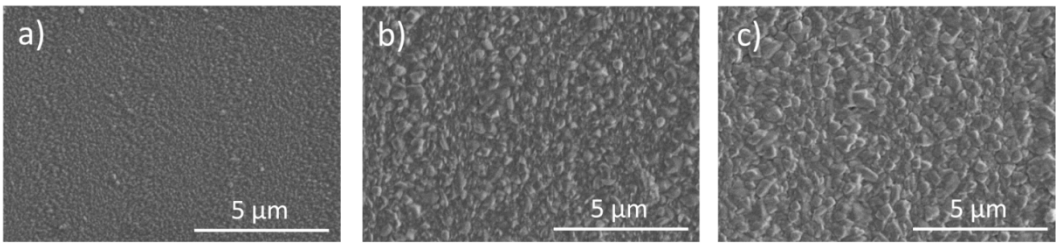

Fig. 2. SEM morphology views of carbon-doped TiO_2 films after a deposition time of a) 60 min, b) 120 min, c) 180 min.

EDS mapping was performed in order to evaluate carbon distribution in TiO_2 films. Fig. 3. shows EDS mapping views of Ti, O, C elements. Fig. 3. shows EDS mapping views of Ti, O, C elements. It is evident that for all samples carbon, titanium and oxygen are uniformly distributed over whole analyzed area of TiO_2 films.

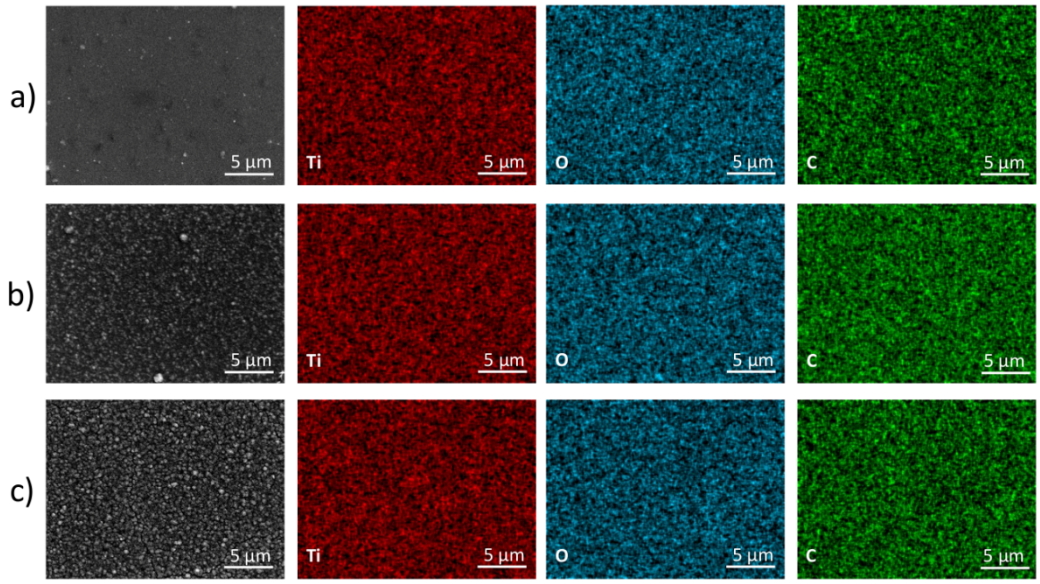

Fig. 3. EDS mapping views of Ti, O, C elements after deposition time of: a) 60 min, b) 120 min, c) 180 min.

In order to reveal more topographic details and obtain quantitative estimation of carbon-doped TiO_2 films surface roughness, AFM measurement was performed. Fig. 4 represents AFM surface images of carbon-doped TiO_2 films which were deposited for 60 min (a), 120 min (b), 180 min (c). Quantitative as well as qualitative AFM data indicates that film surface after 60 min deposition is rather smooth compared to films after longer deposition time: roughness parameters Ra and Rq respectively were 7.6 nm and 11.4 nm for the first sample, 16.0 nm and 20.8 nm for the second, 21.4 nm and 26.2 nm for the third sample. These results agree with the SEM views and thickness measurements and confirm that with the longer deposition time film microstructure evolves into larger grains.

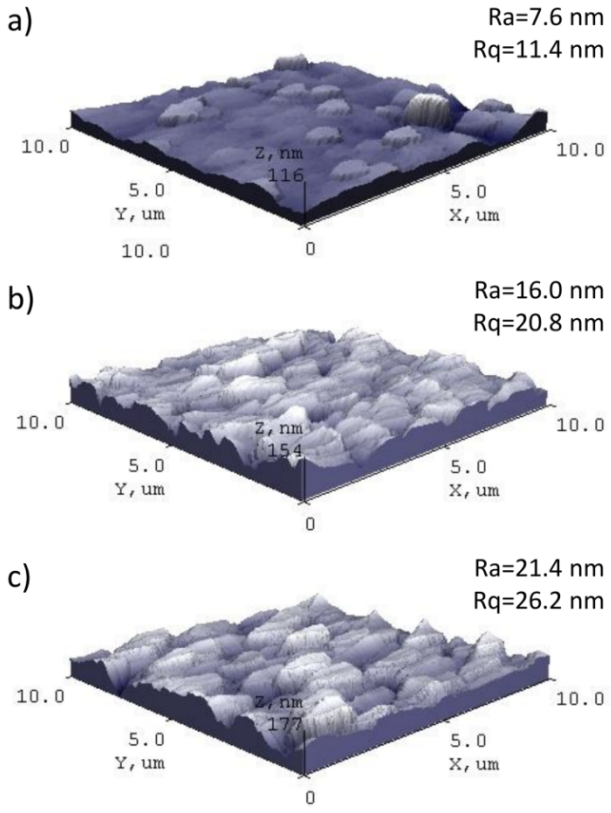

Fig. 4. AFM images of carbon-doped TiO_2 films: a) after 60 min deposition, b) 120 min deposition, c) 180 min deposition.

Table 1. Main characteristics of carbon-doped TiO_2 films.

No.	Deposition time, min	Thickness, nm	Amount of doped carbon, atom. %	Surface roughness, nm		Crystalline size, nm		k value, $\times 10^{-4}$ min^{-1}	
				Ra	Rq	A (101)	R (110)	365 nm	455 nm
1	60	1100	1.65	7.6	11.4	68.8	24.5	10.3	6.7
2	120	2250	2.23	16.0	20.8	55.1	18.0	25.8	7.5
3	180	3325	3.74	21.4	26.2	78.1	12.3	31.8	11.4

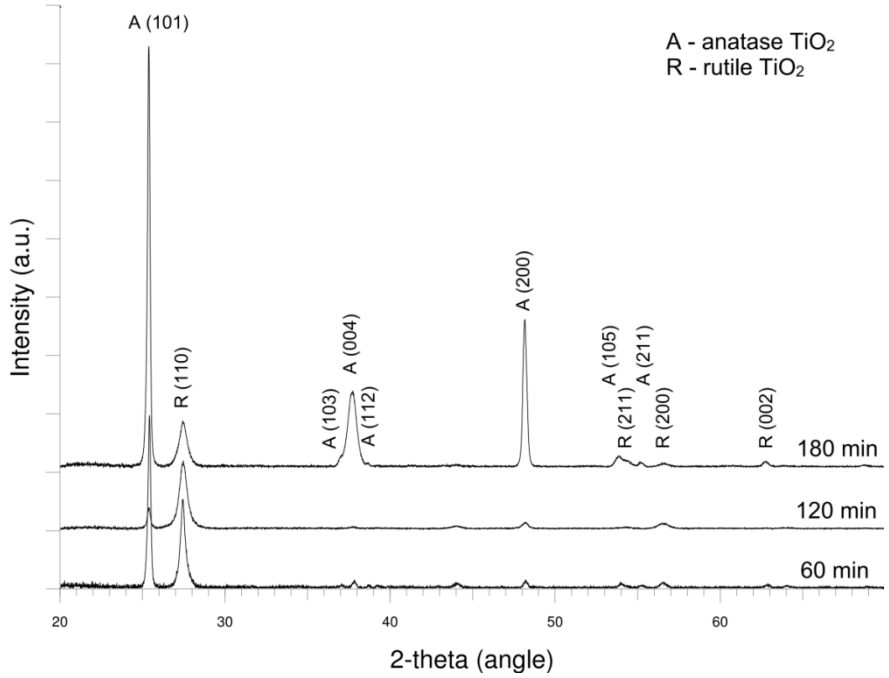

Fig. 5. XRD patterns of carbon-doped TiO_2 films after 60 min, 120 min and 180 min deposition.

Fig. 5. shows the XRD pattern of carbon-doped TiO_2 films after 60 min, 120 min and 180 min deposition time. It was observed that films have polycrystalline TiO_2 structure consisting of anatase (tetragonal, *I41/amd*, JCPDS No. 21-1272) and rutile (tetragonal, *P42/mnm*, JCPDS No. 086-0148) crystalline phases. The most intensive anatase and rutile peaks have (101) and (110) orientation respectively. Notably, it is observed that for shorter deposition times carbon-doped TiO_2 tend to form a relatively strongly oriented film structures whereas with the longer deposition time significantly less textured polycrystalline structure is formed. Similar polycrystalline structure growth results using longer formation time were observed by other authors [52,53]. We suggest that such behavior is related to the competing crystallization of two dissimilar TiO_2 phases. Crystalline sizes were calculated for both anatase (101) and rutile (110) orientations. Anatase (101) orientation showed a tendency to grow (68.8 nm after 60 min and 78.1 nm after 180 min deposition time) while the crystalline size of rutile (110) orientation decrease during deposition

time (from 24.5 nm to 12.3 nm). Moreover, strong anatase (004) and (200) orientations were observed after 180 min deposition time.

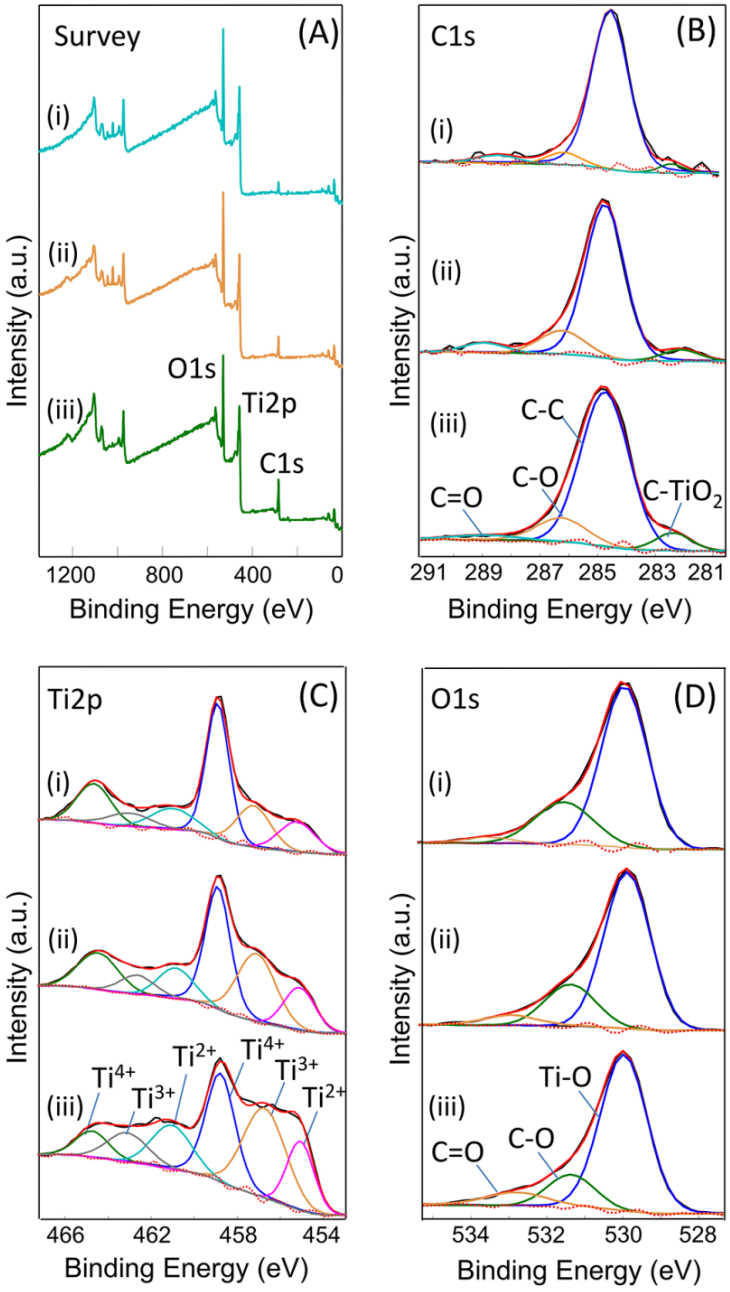

Fig. 6. The XPS spectra of (A) survey, (B) C1s, (C) (Ti2p), and (D) O1s of TiO_2 films after (i) 60 min, (ii) 120 min and (iii) 180 min deposition time.

The chemical state investigation of carbon atoms incorporated into TiO_2 photocatalyst was performed by XPS measurement. Prior to the sample analysis, the surface of carbon doped TiO_2

films was gently pre-cleaned using Ar^+ ions. This allowed to avoid adventitious carbon during the analysis. Nevertheless, strong carbon peak was observed even after pre-cleaning process. Fig. 6. shows the XPS survey (A), C1s (B), Ti2p (C) and O1s (D) spectra of TiO_2 films after different deposition times. The clear evidence of Ti, O and C elements could be seen in survey spectra. It is important to mention that no additional elements or impurities were observed. All survey spectra were very similar; however, some differences were observed by analyzing individual core level spectra of C, Ti and O.

The C1s spectra of all three samples are shown in Fig. 6 (B). In all cases, it consists of four components with the peak energies at approximately 282.2 eV, 284.7 eV, 286.2 eV and 288.9 eV. The peak at 284.7 eV is attributed to C-C bond, which covers nearly 76 % of all C1s peak area. This means that the majority of incorporated carbon does not react and influence TiO_2 states. The other two peaks with the binding energies of 286.2 eV and 288.9 eV belong to C-O/C-OH and C-OH bonds respectively [54]. The last peak of C1s spectra was observed at around 282.2 eV in all three samples. Based on Y. Park et al. if anionic carbon species were doped into TiO_2 lattice the peak would be found at 282 eV which is attributed to C-Ti bond [55]. Moreover, carbon could be doped into TiO_2 lattice by substituting the O site and formed O-Ti-C bond. Due to the electronegativity of carbon which is smaller than oxygen, electron density around Ti atom should be decreased compared to C-Ti bond. This process invokes a small binding energy shift of C-Ti to higher energy [56]. According to this explanation, we assert that carbon has been doped into TiO_2 lattice by forming an O-Ti-C bond ($C\text{-}TiO_2$). C1s peak fitting suggest that the concentration of carbon-doped TiO_2 takes 3.3 %, 5.2 % and 6.8 % of C1s spectra area at (i), (ii) and (iii) samples respectively.

The Ti2p spectra are shown in Fig. 6 (C). Three Ti2p3/2 peaks were observed at binding energies of 455.0 eV, 456.8 eV and 458.7 eV (corresponding Ti2p1/2 are observed at 460.9, 463.0 eV and

464.4 eV) and were attributed to Ti^{2+}, Ti^{3+}, Ti^{4+} respectively. The appearance of Ti^{2+} and Ti^{3+} in TiO_2 lattice is attributed to the Ar^+ sputtering during the XPS measurement [56,57]. The separation between two Ti^{4+} peaks is 5.7 eV. This value agrees with the theoretical difference between these two peaks of titanium dioxide and confirms the existence of TiO_2 compound. Moreover, a small shift of Ti^{4+} was observed to lower energies (standard TiO_2 binding energy is 458.8 eV). The similar shift to lower energies was observed at Ti-O bond in O1s spectra (Fig. 5 (D)). The peak around 529.8 eV was attributed to Ti-O bond (standard binding energy is 529.9 eV). These shifts were invoked by carbon which is doped in TiO_2 lattice and confirm the formation of O-Ti-C bond. Other two peaks were observed at 531.4 eV and 532.9 eV binding energies and corresponded to C-O and C-OH bonds respectively [54].

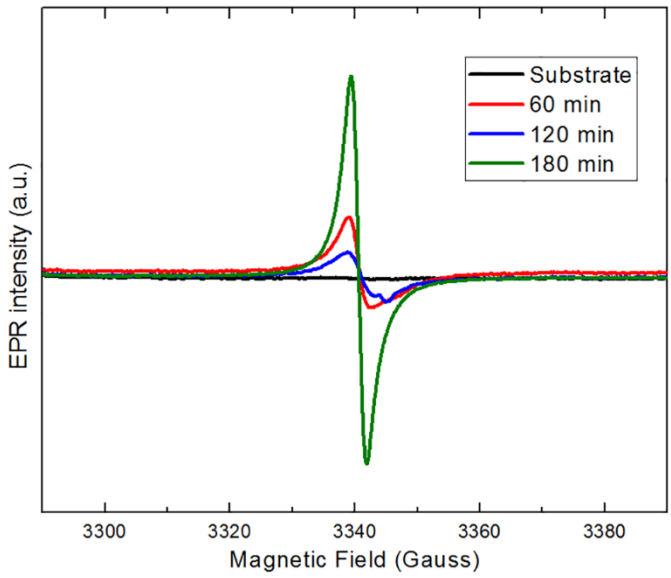

Fig. 7. ESR spectra views of TiO_2 films at room temperature

It is known that atoms or molecules with unpaired electrons have a significant influence in photocatalysis, which can be quantitatively and qualitatively evaluated by ESR [58,59]. Measurements of ESR were performed at room temperature to characterize the unpaired electrons or paramagnetic centers. ESR spectra of the investigated films are shown in Fig. 7. The

results showed that very strong ESR signal at g = 2.003 ± 0.001 was observed by TiO_2 film after 180 min deposition. This could be attributed to the unpaired electron trapped on surface oxygen vacancies [60,61]. Significant weaker signals at about g = 2.001 ± 0.001 were observed for TiO_2 films after 60 min and 120 min deposition respectively. Such significant decrease of ESR spectra intensity implies the reduction of the Ti^{3+} spins. The ESR results demonstrate that longer deposition time may contribute to the generation of oxygen vacancies while TiO_2 is doped by carbon. Similar results were observed by other authors where carbon or other dopants invoke generation of oxygen vacancies in TiO_2 [62–65].

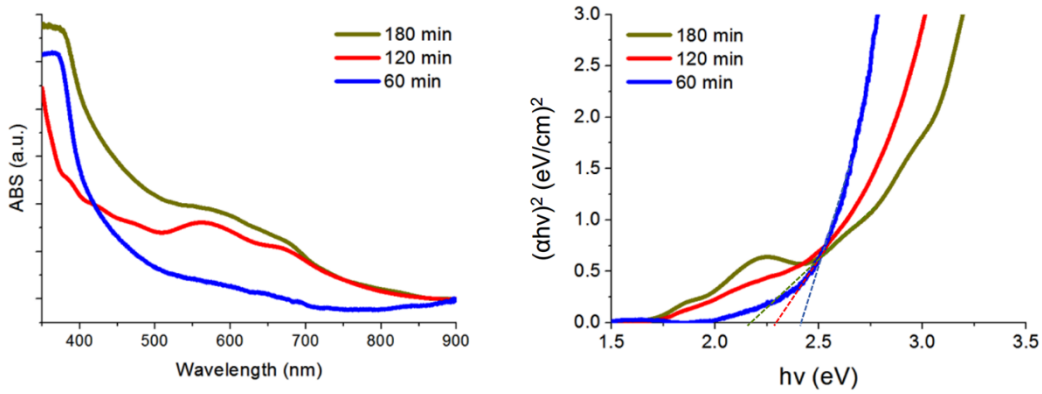

Fig. 8. Optical properties of deposited carbon-doped TiO_2 films: a) VIS-IR absorption spectra of carbon-doped TiO_2 films b) Bang gaps based on Tauc plots.

One of the most important parameters for practical application of black colour carbon-doped TiO_2 is the capability to absorb visible light of solar spectra [27,33]. The VIS-IR absorption spectra of carbon-doped TiO_2 films after 60 min, 120 min and 180 min (black colour TiO_2) deposition time are shown in Fig. 8. Results showed that all black colour TiO_2 films have promising absorption characteristics in visible light spectra. The redshift of absorption onset was observed in all samples compared to compared to commercially available TiO2 P25 degussa powders [66]. Moreover, the significant absorption in the range between 400 nm and 700 nm was observed for TiO_2 films deposited 120 and 180 min respectively. Similar results were observed by W. Hui et al., which

incorporated Cu particles into heterojunction rutile/anatase phase TiO_2 films. They claimed that higher visible light absorption is related to the reduction of TiO_2 band gap [67]. Moreover, similar results were observed by other authors, which analyzed carbon-doped TiO_2 photocatalyst [55,56,66,68,69].

The optical band gaps of deposited carbon-doped TiO_2 films were obtained using Tauc plots, following procedure described in paper of S. Kumal et al [70]. It was evaluated that the optical band gap of transparent TiO_2 film was about 3.3 eV while optical band gap of black colour TiO_2 films varied from approximately 2.2 eV to 2.4 eV, according to Fig.8, b. This indicates that the formation of carbon-doped TiO_2 during magnetron sputtering influence reduction of its optical band gap. This could be the main reason for improved visible light absorption.

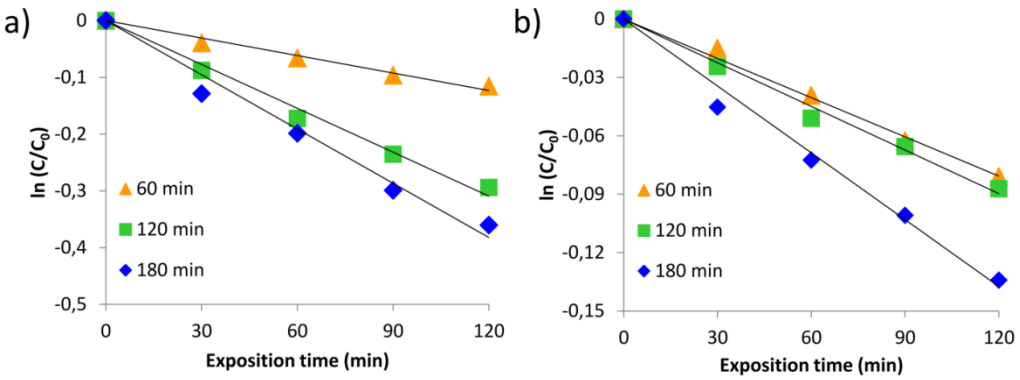

Fig. 9. Photocatalytic degradation kinetics of MB dye by TiO_2 films irradiated with a) 365 nm wavelength and b) 455 nm wavelength irradiation.

Decomposition of MB solution by carbon-doped TiO_2 films irradiated with UV-A (365 nm) and visible light (455 nm) irradiation are shown in Fig. 9. (a) and Fig. 9. (b). Also, the rate constants of MB photocatalytic degradation (first-order reaction constants, k values) for carbon-doped TiO_2 films with different deposition time were extracted from linear fitting of the curves variation of $\ln(C/C_0)$ with exposition time (table 1). It is important to note that the rate of MB absorption by carbon-doped TiO_2 films and MB bleaching under UV-A and visible light without photocatalyst

were negligible (k values < 1×10^{-4} min^{-1}). Accordingly, this data was not included in Fig. 9. and table 1.

Results of MB bleaching experiment showed that all deposited carbon-doped TiO_2 films exhibit photocatalytic decomposition properties. The highest decomposition rate was observed by using carbon-doped TiO_2 film after 180 min deposition time (k values 3.18×10^{-3} min^{-1} with UV-A and 1.14×10^{-3} min^{-1} with visible 455 nm light irradiation) while the lowest decomposition ratio was observed by carbon-doped TiO_2 films after 60 min deposition time (k values 1.03×10^{-3} min^{-1} with UV-A and 0.67×10^{-3} min^{-1} with visible 455 nm light irradiation). These photocatalytic decomposition properties could be related to several processes. First of all, XRD analysis showed that deposited carbon-doped TiO_2 films have both anatase and rutile crystalline phases. A lot of researchers claimed that heterojunction of two phases have synergistic effects and can improve the photocatalytic activity compared to pure TiO_2 phases. Normally, by absorbing light electrons are excited from the valence band to the conduction band of the same material and fall-back to the valence band during electron-hole recombination. Anatase has wider band gap compared to rutile [15], therefore at the heterojunction electron also can jump from conduction/valence band of anatase to conduction/valence band of rutile. This means that at heterojunction, electrons can spend more time at “unified” conduction band and sometimes have no space for the relaxation to the valence band. Altogether this reduces the possibility of electron-hole recombination [71,72]. Moreover, different orientations of the same phase also have different photocatalysis characteristics which could also have a positive influence on photocatalysis [73]. X. Wang et. all showed that higher anatase TiO_2 crystalline size have a positive influence on its photocatalytic properties [74]. The similar results were observed in the presented case where the highest photocatalytic activity was observed using carbon-doped TiO_2 film after 180 min deposition (anatase TiO_2 crystalline size 78.1 nm, see table 1). Higher surface roughness resulting in higher

specific surface area, as well as larger crystallite size, could also have positive effect on photocatalytic activity. Higher roughness determines higher active contact area between TiO_2 film and tested solution [74]. Finally, incorporation of carbon into TiO_2 film and formation of carbon-doped TiO_2 phase allowed to reduce its band gap, change its colour from transparent to black and as a consequence to improve visible light absorption properties. Arguably the lowering of the band gap was the most important advancement in order to form TiO_2 films which are photocatalytically active under visible light (455 nm) irradiation.

4. Conclusions

Black colour anatase/rutile heterostructure carbon doped TiO_2 films (1.65 at. % to 3.74 at. % carbon) were deposited using is-situ DC magnetron sputtering technique. Throughout analysis of the films showed that TiO_2 film thickness, surface roughness and crystalline size increase with the longer deposition time. XPS analysis confirmed carbon incorporation into the TiO_2 film. ESR demonstrated generation of oxygen vacancies where unpaired electron was trapped. Analysis of the optical properties of the carbon-doped TiO_2 films revealed that incorporation of carbon during deposition process can reduce the optical band gap of TiO_2 from approximately 3.3 eV to 2.2-2.4 eV. Accordingly, MB bleaching experiment showed that black colour TiO_2 films exhibit significant photocatalytic activity under both UV-A (365 nm) and visible light (455 nm) irradiation. The highest MB decomposition rates were observed for carbon-doped TiO_2 film after 180 min deposition time, where the first order reaction constants were 3.18×10^{-3} min^{-1} with UV-A and 1.14×10^{-3} min^{-1} with visible 455 nm light irradiation respectively. These results showed that such black colour TiO_2 formation technique has promising characteristics for further photocatalytically active TiO_2 formation.

Acknowledgement

This research is funded by the European Social Fund according to the activity ‘Improvement of researchers’ qualification by implementing world-class R&D projects’ of Measure No. 09.3.3-LMT-K-712, project „Investigation of the application of TiO_2 and ZnO for the visible light assisted photocatalytical disinfection of the biologically contaminated water“ (09.3.3-LMT-K-712-01-0175). The authors express gratitude for the S. Tuckute, M. Urbonavicius, G. Laukaitis and K. Bockute for their valuable input in current work.

References

[1] Y. Zhang, Z. Jiang, J. Huang, L.Y. Lim, W. Li, J. Deng, D. Gong, Y. Tang, Y. Lai, Z. Chen, Titanate and titania nanostructured materials for environmental and energy applications: a review, RSC Adv. 5 (2015) 79479–79510. doi:10.1039/C5RA11298B.

[2] P.V. Laxma Reddy, B. Kavitha, P.A. Kumar Reddy, K.H. Kim, TiO2-based photocatalytic disinfection of microbes in aqueous media: A review, Environ. Res. 154 (2017) 296–303. doi:10.1016/j.envres.2017.01.018.

[3] B. Srikanth, R. Goutham, R. Badri Narayan, A. Ramprasath, K.P. Gopinath, A.R. Sankaranarayanan, Recent advancements in supporting materials for immobilised photocatalytic applications in waste water treatment, J. Environ. Manage. 200 (2017) 60–78. doi:10.1016/j.jenvman.2017.05.063.

[4] H. Park, Y. Park, W. Kim, W. Choi, Surface modification of TiO2 photocatalyst for environmental applications, J. Photochem. Photobiol. C Photochem. Rev. 15 (2013) 1–20. doi:10.1016/j.jphotochemrev.2012.10.001.

[5] T. Tasaki, T. Wada, K. Fujimoto, S. Kai, K. Ohe, T. Oshima, Y. Baba, M. Kukizaki, Degradation of methyl orange using short-wavelength UV irradiation with oxygen microbubbles, J. Hazard. Mater. 162 (2009) 1103–1110. doi:10.1016/j.jhazmat.2008.05.162.

[6] C. Kim, J.T. Kim, K.S. Kim, S. Jeong, H.Y. Kim, Y.S. Han, Immobilization of TiO2on an ITO substrate to facilitate the photoelectrochemical degradation of an organic dye pollutant, Electrochim. Acta. 54 (2009) 5715–5720. doi:10.1016/j.electacta.2009.05.018.

[7] M.R.D. Khaki, M.S. Shafeeyan, A.A.A. Raman, W.M.A.W. Daud, Application of doped photocatalysts for organic pollutant degradation - A review, J. Environ. Manage. 198 (2017) 78–94. doi:10.1016/j.jenvman.2017.04.099.

[8] N. Daneshvar, S. Aber, M.S. Seyed Dorraji, A.R. Khataee, M.H. Rasoulifard, Photocatalytic degradation of the insecticide diazinon in the presence of prepared nanocrystalline ZnO powders under irradiation of UV-C light, Sep. Purif. Technol. 58 (2007) 91–98. doi:10.1016/j.seppur.2007.07.016.

[9] Y. Abdollahi, A.H. Abdullah, Z. Zainal, N.A. Yusof, Photodegradation of m-cresol by Zinc Oxide under Visible-light Irradiation, Int. J. Chem. 3 (2011) 31–43. doi:10.5539/ijc.v3n3p31.

[10] S.Y. Lee, S.J. Park, TiO2 photocatalyst for water treatment applications, J. Ind. Eng. Chem. 19 (2013) 1761–1769. doi:10.1016/j.jiec.2013.07.012.

[11] A. Fujishima, X. Zhang, D.A. Tryk, TiO2 photocatalysis and related surface phenomena, Surf. Sci. Rep. 63 (2008) 515–582. doi:10.1016/j.surfrep.2008.10.001.

[12] V. Likodimos, Photonic crystal-assisted visible light activated TiO2 photocatalysis, Appl. Catal. B Environ. 230 (2018) 269–303. doi:10.1016/j.apcatb.2018.02.039.

[13] H. Abdullah, M.M.R. Khan, H.R. Ong, Z. Yaakob, Modified TiO2 photocatalyst for CO2 photocatalytic reduction: An overview, J. CO2 Util. 22 (2017) 15–32. doi:10.1016/j.jcou.2017.08.004.

[14] S. Varnagiris, M. Urbonavicius, S. Tuckute, M. Lelis, D. Milcius, Development of photocatalytically active TiO2 thin films on expanded polystyrene foam using magnetron sputtering, Vacuum. 143 (2017) 28–35. doi:10.1016/j.vacuum.2017.05.031.

[15] M. Pelaez, N.T. Nolan, S.C. Pillai, M.K. Seery, P. Falaras, A.G. Kontos, P.S.M. Dunlop, J.W.J. Hamilton,

J.A. Byrne, K. O'Shea, M.H. Entezari, D.D. Dionysiou, A review on the visible light active titanium dioxide photocatalysts for environmental applications, Appl. Catal. B Environ. 125 (2012) 331–349. doi:10.1016/j.apcatb.2012.05.036.

[16] W. Fang, M. Xing, J. Zhang, Modifications on reduced titanium dioxide photocatalysts: A review, J. Photochem. Photobiol. C Photochem. Rev. 32 (2017) 21–39. doi:10.1016/j.jphotochemrev.2017.05.003.

[17] L. Kong, C. Wang, H. Zheng, X. Zhang, Y. Liu, Defect-Induced Yellow Color in Nb-Doped TiO2 and Its Impact on Visible-Light Photocatalysis, J. Phys. Chem. C. 119 (2015) 16623–16632. doi:10.1021/acs.jpcc.5b03448.

[18] S. Sakthivel, M. Janczarek, H. Kisch, Visible light activity and photoelectrochemical properties of nitrogen-doped TiO2, J. Phys. Chem. B. 108 (2004) 19384–19387. doi:10.1021/jp046857q.

[19] J. Zhao, L. Zhang, W. Xing, K. Lu, A novel method to prepare B/N codoped anatase TiO2, J. Phys. Chem. C. 119 (2015) 7732–7737. doi:10.1021/jp512837n.

[20] G. Liu, L.-C. Yin, J. Wang, P. Niu, C. Zhen, Y. Xie, H.-M. Cheng, A red anatase TiO2 photocatalyst for solar energy conversion, Energy Environ. Sci. 5 (2012) 9603. doi:10.1039/c2ee22930g.

[21] Y. Zhou, C. Chen, N. Wang, Y. Li, H. Ding, Stable Ti^{3+} Self-Doped Anatase-Rutile Mixed TiO_2 with Enhanced Visible Light Utilization and Durability, J. Phys. Chem. C. 120 (2016) 6116–6124. doi:10.1021/acs.jpcc.6b00655.

[22] J. Zheng, Y. Liu, G. Ji, P. Zhang, X. Cao, B. Wang, C. Zhang, X. Zhou, Y. Zhu, D. Shi, Hydrogenated Oxygen-Deficient Blue Anatase as Anode for High-Performance Lithium Batteries, ACS Appl. Mater. Interfaces. 7 (2015) 23431–23438. doi:10.1021/acsami.5b07000.

[23] G. Li, Z. Zhang, H. Peng, K. Chen, Mesoporous hydrogenated TiO2 microspheres for high rate capability lithium ion batteries, RSC Adv. 3 (2013) 11507. doi:10.1039/c3ra41858h.

[24] B. Kim, Highly Enhanced Photoactivity of Anatase TiO2 Nanocrystals by Controlled Hydrogenation-Induced Surface Defects Highly Enhanced Photoactivity of Anatase TiO2 Nanocrystals by Controlled Hydrogenation-Induced Surface Defects, (2013). doi:10.1021/cs4005776.

[25] M. Wang, B. Nie, K.-K. Yee, H. Bian, C. Lee, H.K. Lee, B. Zheng, J. Lu, L. Luo, Y.Y. Li, Low-temperature fabrication of brown TiO2 with enhanced photocatalytic activities under visible light, Chem. Commun. 52 (2016) 2988–2991. doi:10.1039/C5CC09176D.

[26] M. Xing, J. Zhang, B. Qiu, B. Tian, M. Anpo, M. Che, A brown mesoporous TiO2-x/MCF composite with an extremely high quantum yield of solar energy photocatalysis for H2evolution, Small. 11 (2015) 1920–1929. doi:10.1002/smll.201403056.

[27] S.G. Ullattil, S.B. Narendranath, S.C. Pillai, P. Periyat, Black TiO2Nanomaterials: A Review of Recent Advances, Chem. Eng. J. 343 (2018) 708–736. doi:10.1016/j.cej.2018.01.069.

[28] M. Coto, G. Divitini, A. Dey, S. Krishnamurthy, N. Ullah, C. Ducati, R.V. Kumar, Tuning the properties of a black TiO2-Ag visible light photocatalyst produced by a rapid one-pot chemical reduction, Mater. Today Chem. 4 (2017) 142–149. doi:10.1016/j.mtchem.2017.03.002.

[29] S. Chen, Y. Wang, J. Li, Z. Hu, H. Zhao, W. Xie, Z. Wei, Synthesis of black TiO2 with efficient visible-light photocatalytic activity by ultraviolet light irradiation and low temperature annealing, Mater. Res. Bull. 98 (2018) 280–287. doi:10.1016/j.materresbull.2017.10.036.

[30] L. Xin, X. Liu, Black TiO2 inverse opals for visible-light photocatalysis, RSC Adv. 5 (2015) 71547–71550. doi:10.1039/C5RA10280D.

[31] J. Dong, J. Han, Y. Liu, A. Nakajima, S. Matsushita, S. Wei, W. Gao, Defective black TiO2 synthesized via anodization for visible-light photocatalysis, ACS Appl. Mater. Interfaces. 6 (2014) 1385–1388. doi:10.1021/am405549p.

[32] C. Sun, Y. Jia, X.H. Yang, H.G. Yang, X. Yao, G.Q. Lu, A. Selloni, S.C. Smith, Hydrogen incorporation and storage in well-defined nanocrystals of anatase titanium dioxide, J. Phys. Chem. C. 115 (2011) 25590–25594. doi:10.1021/jp210472p.

[33] X. Chen, L. Liu, P.Y. Yu, S.S. Mao, Increasing solar absorption for photocatalysis with black hydrogenated titanium dioxide nanocrystals, Science (80-.). 331 (2011) 746–750. doi:10.1126/science.1200448.

[34] T. Leshuk, S. Linley, F. Gu, Hydrogenation processing of TiO2 nanoparticles, Can. J. Chem. Eng. 91 (2013) 799–807. doi:10.1002/cjce.21745.

[35] A. Sinhamahapatra, J.-P. Jeon, J.-S. Yu, A new approach to prepare highly active and stable black titania for visible light-assisted hydrogen production, Energy Environ. Sci. 8 (2015) 3539–3544. doi:10.1039/C5EE02443A.

[36] Y. Zhu, D. Liu, M. Meng, H2 spillover enhanced hydrogenation capability of TiO2 used for photocatalytic splitting of water: a traditional phenomenon for new applications, Chem. Commun. 50 (2014) 6049–6051. doi:10.1039/C4CC01667J.

[37] L. Han, Z. Ma, Z. Luo, G. Liu, J. Ma, X. An, Enhanced visible light and photocatalytic performance of TiO2 nanotubes by hydrogenation at lower temperature, RSC Adv. 6 (2016) 6643–6650. doi:10.1039/C5RA11616C.

[38] Z. Wang, C. Yang, T. Lin, H. Yin, P. Chen, D. Wan, F. Xu, F. Huang, J. Lin, X. Xie, M. Jiang, H-doped black titania with very high solar absorption and excellent photocatalysis enhanced by localized surface plasmon resonance, Adv. Funct. Mater. 23 (2013) 5444–5450. doi:10.1002/adfm.201300486.

[39] Y. Yan, M. Han, A. Konkin, T. Koppe, D. Wang, T. Andreu, G. Chen, U. Vetter, J.R. Morante, P. Schaaf, Slightly hydrogenated TiO_2 with enhanced photocatalytic performance, J. Mater. Chem. A. 2 (2014) 12708–12716. doi:10.1039/C4TA02192D.

[40] Z. Wang, C. Yang, T. Lin, H. Yin, P. Chen, D. Wan, F. Xu, F. Huang, J. Lin, X. Xie, M. Jiang, Visible-light photocatalytic, solar thermal and photoelectrochemical properties of aluminium-reduced black titania, Energy Environ. Sci. 6 (2013) 3007. doi:10.1039/c3ee41817k.

[41] H. Cui, W. Zhao, C. Yang, H. Yin, T. Lin, Y. Shan, Y. Xie, H. Gu, F. Huang, Black TiO2 nanotube arrays for high-efficiency photoelectrochemical water-splitting, J. Mater. Chem. A. 2 (2014) 8612–8616. doi:10.1039/C4TA00176A.

[42] S. Chen, J. Tao, H. Tao, C. Wang, Y. Shen, J. Jiang, L. Zhu, X. Zeng, T. Wang, One-Step Solvothermal Synthesis of Black TiO2 Films for Enhanced Visible Absorption, J. Nanosci. Nanotechnol. 16 (2016) 3146–3149. doi:10.1166/jnn.2016.10864.

[43] H. Zhou, Y. Zhang, Electrochemically Self-Doped TiO2 Nanotube Arrays for Supercapacitors, J. Phys. Chem. C. 118 (2014) 5626–5636. doi:10.1021/jp4082883.

[44] P.. Kelly, R.. Arnell, Magnetron sputtering: a review of recent developments and applications, Vacuum. 56 (2000) 159–172. doi:10.1016/S0042-207X(99)00189-X.

[45] J. Šícha, D. Heřman, J. Musil, Z. Strýhal, J. Pavlik, Surface morphology of magnetron sputtered TiO2 films, Plasma Process. Polym. 4 (2007) 345–349. doi:10.1002/ppap.200730906.

[46] P.J. Kelly, G.T. West, M. Ratova, L. Fisher, S. Ostovarpour, J. Verran, Structural formation and photocatalytic activity of magnetron sputtered titania and doped-titania coatings, Molecules. 19 (2014) 16327–16348. doi:10.3390/molecules191016327.

[47] R. Klaysri, M. Ratova, P. Praserthdam, P. Kelly, Deposition of Visible Light-Active C-Doped Titania Films via Magnetron Sputtering Using CO2 as a Source of Carbon, Nanomaterials. 7 (2017) 113. doi:10.3390/nano7050113.

[48] D. Xie, F. Wen, W. Yang, X. Li, Y. Leng, G. Wan, H. Sun, N. Huang, Carbon-doped titanium oxide films by DC reactive magnetron sputtering using CO2 and O2 as reactive gas, Acta Metall. Sin. (English Lett. 27 (2014) 239–244. doi:10.1007/s40195-014-0049-z.

[49] F. Wen, C. Zhang, D. Xie, H. Sun, Y.X. Leng, Research of composition and photocatalytic property of carbon-doped Ti-O films prepared by R-MS using CO 2 gas resource, Nucl. Instruments Methods Phys. Res. Sect. B Beam Interact. with Mater. Atoms. 307 (2013) 381–384. doi:10.1016/j.nimb.2012.11.080.

[50] M. Ratova, R. Klaysri, P. Praserthdam, P.J. Kelly, Visible light active photocatalytic C-doped titanium dioxide films deposited via reactive pulsed DC magnetron co-sputtering: Properties and photocatalytic activity, Vacuum. 149 (2018) 214–224. doi:10.1016/j.vacuum.2018.01.003.

[51] D. Mitoraj, U. Lamdab, W. Kangwansupamonkon, M. Pacia, W. Macyk, N. Wetchakun, R. Beranek, Revisiting the problem of using methylene blue as a model pollutant in photocatalysis: The case of InVO4/BiVO4 composites, J. Photochem. Photobiol. A Chem. 366 (2018) 103–110. doi:10.1016/j.jphotochem.2018.02.023.

[52] M.K. Lee, Y.C. Park, Super-hydrophilic anatase TiO2thin film in-situ deposited by DC magnetron sputtering, Thin Solid Films. 638 (2017) 9–16. doi:10.1016/j.tsf.2017.07.046.

[53] M. Rezazadeh Sefideh, Z. Sadeghian, A. Nemati, S.P. Mohammadi, M. Mozafari, Effects of processing conditions on the physico-chemical characteristics of titanium dioxide ultra-thin films deposited by DC magnetron sputtering, Ceram. Int. 41 (2015) 7977–7981. doi:10.1016/j.ceramint.2015.02.142.

[54] NIST, NIST X-ray photoelectron spectroscopy database, NIST standard reference database 20, Version 4.1., (2017).

[55] Y. Park, W. Kim, H. Park, T. Tachikawa, T. Majima, W. Choi, Carbon-doped TiO2 photocatalyst synthesized without using an external carbon precursor and the visible light activity, Appl. Catal. B Environ. 91 (2009) 355–361. doi:10.1016/j.apcatb.2009.06.001.

[56] X. Wu, S. Yin, Q. Dong, C. Guo, H. Li, T. Kimura, T. Sato, Synthesis of high visible light active carbon doped TiO2 photocatalyst by a facile calcination assisted solvothermal method, Appl. Catal. B Environ. 142–143 (2013) 450–457. doi:10.1016/j.apcatb.2013.05.052.

[57] R. Beranek, H. Kisch, Tuning the optical and photoelectrochemical properties of surface-modified TiO2, Photochem. Photobiol. Sci. 7 (2007) 40–48. doi:10.1039/b711658f.

[58] R. Qian, H. Zong, J. Schneider, G. Zhou, T. Zhao, Y. Li, J. Yang, D.W. Bahnemann, J.H. Pan, Charge carrier trapping, recombination and transfer during TiO2 photocatalysis: An overview, Catal. Today. (2018). doi:10.1016/j.cattod.2018.10.053.

[59] M.E. Khan, M.M. Khan, B.K. Min, M.H. Cho, Microbial fuel cell assisted band gap narrowed TiO 2 for

visible lightinduced photocatalytic activities and power generation, Sci. Rep. 8 (2018) 1–12. doi:10.1038/s41598-018-19617-2.

[60] Y. Duan, M. Zhang, L. Wang, F. Wang, L. Yang, X. Li, C. Wang, Plasmonic Ag-TiO 2 − x nanocomposites for the photocatalytic removal of NO under visible light with high selectivity: The role of oxygen vacancies, Appl. Catal. B Environ. 204 (2017) 67–77. doi:10.1016/j.apcatb.2016.11.023.

[61] M. Wajid Shah, Y. Zhu, X. Fan, J. Zhao, Y. Li, S. Asim, C. Wang, Facile Synthesis of Defective TiO 2-x Nanocrystals with High Surface Area and Tailoring Bandgap for Visible-light Photocatalysis, Sci. Rep. 5 (2015) 1–8. doi:10.1038/srep15804.

[62] A.I. Kokorin, A.A. Sukhanov, O.I. Gromov, V.M. Arakelyan, V.M. Aroutiounian, V.K. Voronkova, EPR Study of TiO 2 (Rutile) Doped with Vanadium, Appl. Magn. Reson. 47 (2016) 479–485. doi:10.1007/s00723-016-0762-z.

[63] H. Jiang, J. Liu, M. Li, L. Tian, G. Ding, P. Chen, X. Luo, Facile synthesis of C-decorated Fe, N co-doped TiO 2 with enhanced visible-light photocatalytic activity by a novel co-precursor method, Cuihua Xuebao/Chinese J. Catal. 39 (2018) 747–759. doi:10.1016/S1872-2067(18)63038-4.

[64] Y.N. Li, J. Su, X.Y. Lv, Y.F. Long, H. Yu, R.R. Huang, Y.C. Xie, Y.X. Wen, Zn2+ doped TiO2/C with enhanced sodium-ion storage properties, Ceram. Int. 43 (2017) 10326–10332. doi:10.1016/j.ceramint.2017.05.063.

[65] E.A. Konstantinova, A.I. Kokorin, S. Sakthivel, H. Kisch, K. Lips, Carbon-Doped Titanium Dioxide: Visible Light Photocatalysis and EPR Investigation, Chim. Int. J. Chem. 61 (2008) 810–814. doi:10.2533/chimia.2007.810.

[66] Y. Yang, D. Ni, Y. Yao, Y. Zhong, Y. Ma, J. Yao, High photocatalytic activity of carbon doped TiO2 prepared by fast combustion of organic capping ligands, RSC Adv. 5 (2015) 93635–93643. doi:10.1039/C5RA19058D.

[67] W. Hui, S. Guodong, Z. Xiaoshu, Z. Wei, H. Lin, Y. Ying, In-situ synthesis of TiO2 rutile/anatase heterostructure by DC magnetron sputtering at room temperature and thickness effect of outermost rutile layer on photocatalysis, J. Environ. Sci. 60 (2017) 33–42. doi:10.1016/j.jes.2017.02.019.

[68] J. Shao, W. Sheng, M. Wang, S. Li, J. Chen, Y. Zhang, S. Cao, In situ synthesis of carbon-doped TiO2 single-crystal nanorods with a remarkably photocatalytic efficiency, Appl. Catal. B Environ. 209 (2017) 311–319. doi:10.1016/j.apcatb.2017.03.008.

[69] G. Wu, T. Nishikawa, B. Ohtani, A. Chen, Synthesis and Characterization of Carbon-Doped TiO2 Nanostructures with Enhanced Visible Light Response, Chem. Mater. 19 (2007) 4530–4537. doi:10.1021/cm071244m.

[70] S. Kumar, V. Singh, A. Tanwar, Structural, morphological, optical and photocatalytic properties of Ag-doped ZnO nanoparticles, J. Mater. Sci. Mater. Electron. 27 (2016) 2166–2173. doi:10.1007/s10854-015-4227-1.

[71] C. Byrne, G. Subramanian, S.C. Pillai, Recent advances in photocatalysis for environmental applications, J. Environ. Chem. Eng. (2017) 0–1. doi:10.1016/j.jece.2017.07.080.

[72] T. Ohno, K. Tokieda, S. Higashida, M. Matsumura, Synergism between rutile and anatase TiO2 particles in photocatalytic oxidation of naphthalene, Appl. Catal. A Gen. 244 (2003) 383–391. doi:10.1016/S0926-860X(02)00610-5.

[73] T. Luttrell, S. Halpegamage, J. Tao, A. Kramer, E. Sutter, M. Batzill, Why is anatase a better photocatalyst than rutile? Model studies on epitaxial TiO2 films, Sci. Rep. 4 (2014) 4043. doi:10.1038/srep04043.

[74] X. Wang, L. Sø, R. Su, S. Wendt, P. Hald, A. Mamakhel, C. Yang, Y. Huang, B.B. Iversen, F. Besenbacher, The influence of crystallite size and crystallinity of anatase nanoparticles on the photo-degradation of phenol, J. Catal. 310 (2014) 100–108. doi:10.1016/j.jcat.2013.04.022.

Institute of Solid State Physics, University of Latvia as the Center of Excellence has received funding from the European Union's Horizon 2020 Framework Programme H2020-WIDESPREAD-01-2016-2017-TeamingPhase2 under grant agreement No. 739508, project CAMART²

Figure Captions

Fig. 1. Scheme of experimental set-up during carbon-doped TiO_2 formation

Fig. 2. SEM morphology views of carbon-doped TiO_2 films after a deposition time of a) 60 min, b) 120 min, c) 180 min

Fig. 3. EDS mapping views of Ti, O, C elements after deposition time of: a) 60 min, b) 120 min, c) 180 min.

Fig. 4. AFM images of carbon-doped TiO_2 films: a) after 60 min deposition, b) 120 min deposition, c) 180 min deposition

Fig. 5. XRD patterns of carbon-doped TiO_2 films after 60 min, 120 min and 180 min deposition time

Fig. 6. The XPS spectra of (A) survey, (B) C1s, (C) (Ti2p), and (D) O1s of TiO_2 films after (i) 60 min, (ii) 120 min and (iii) 180 min deposition time

Fig. 7. EPR spectra views of TiO2 films at room temperature

Fig. 8. Optical properties of deposited carbon-doped TiO_2 films: a) VIS-IR absorption spectra of carbon-doped TiO_2 films b) Bang gaps based on Tauc plots

Fig. 9. Photocatalytic degradation kinetics of MB dye by TiO_2 films irradiated with a) 365 nm wavelength and b) 455 nm wavelength irradiation

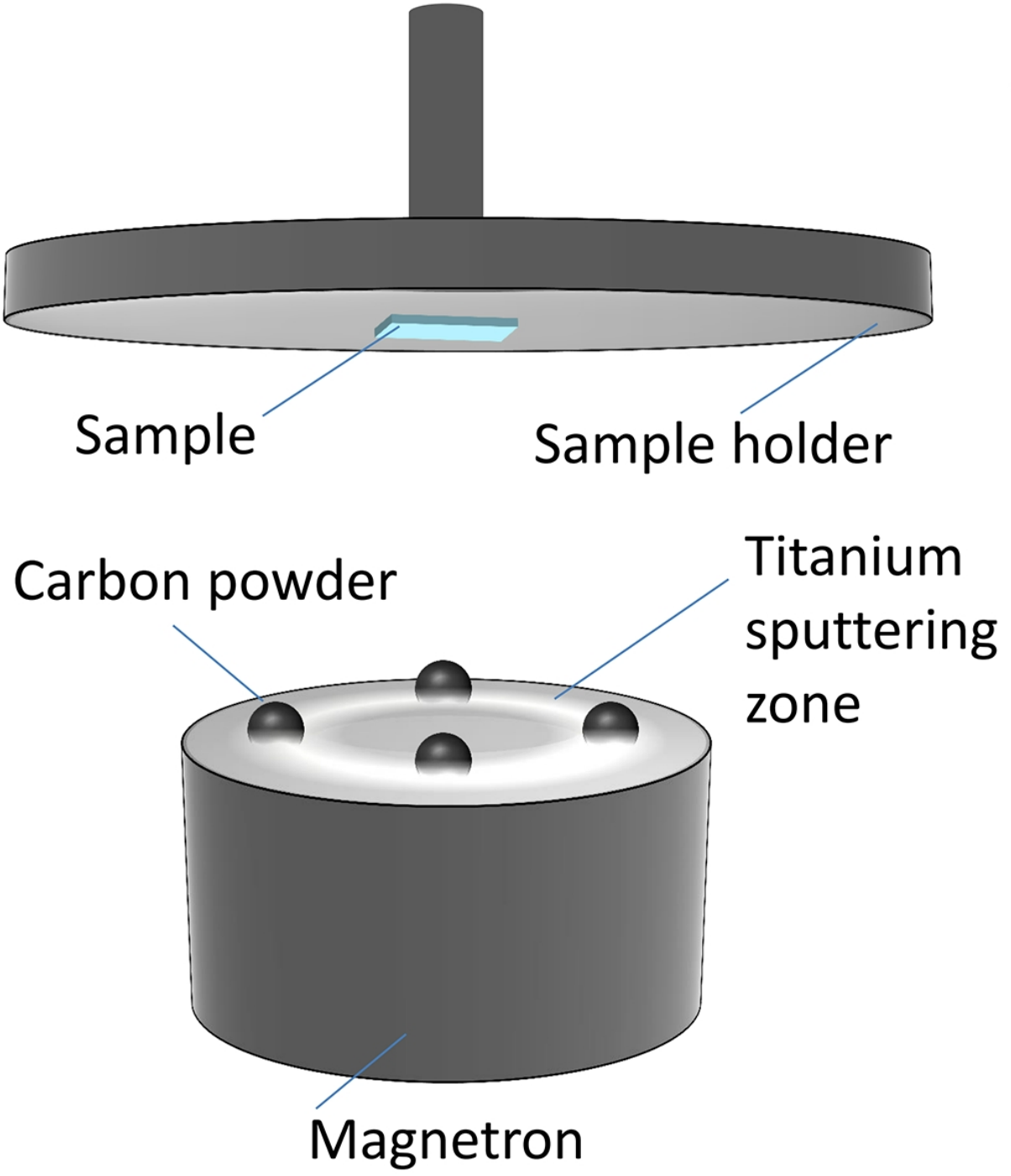
Sample
Sample holder
Carbon powder
Titanium sputtering zone
Magnetron

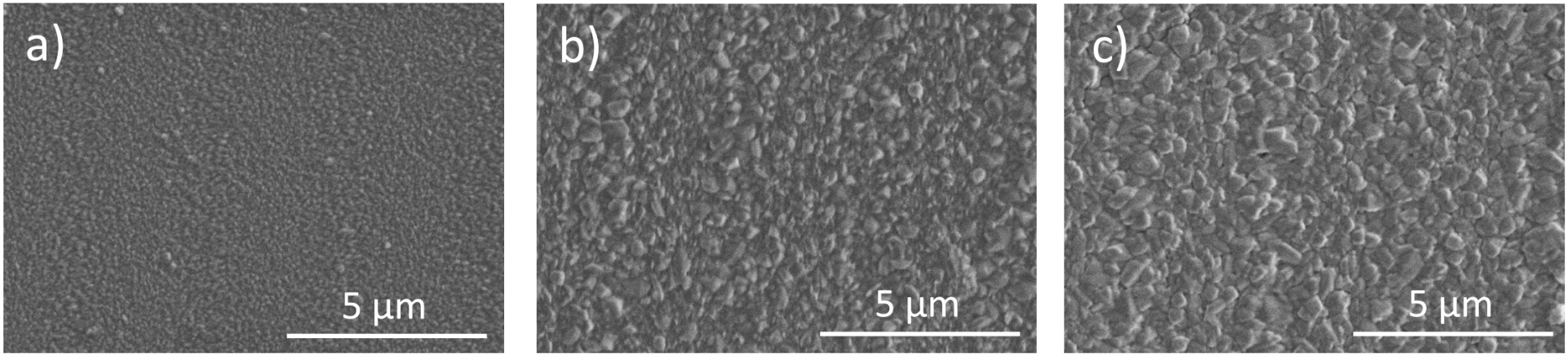
a)
5 µm
b)
5 µm
c)
5 µm

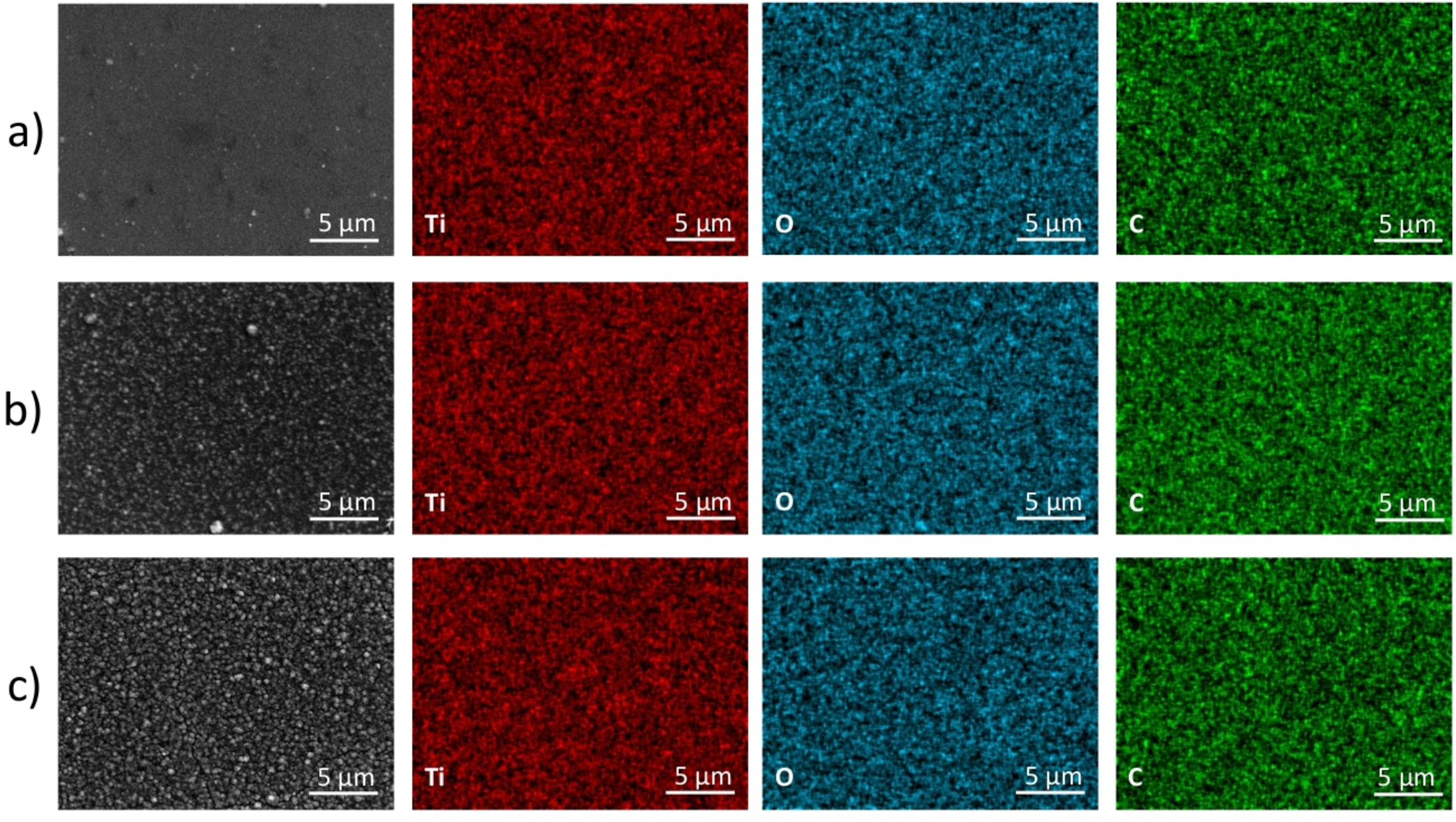
a)
5 µm
Ti
5 µm
O
5 µm
C
5 µm
b)
5 µm
Ti
5 µm
O
5 µm
C
5 µm
c)
5 µm
Ti
5 µm
O
5 µm
C
5 µm

a)

Ra=7.6 nm
Rq=11.4 nm

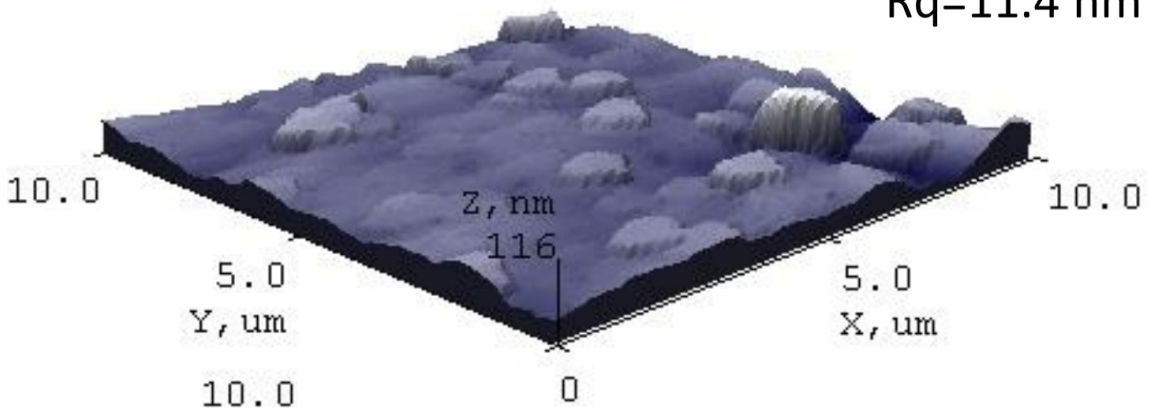

b)

Ra=16.0 nm
Rq=20.8 nm

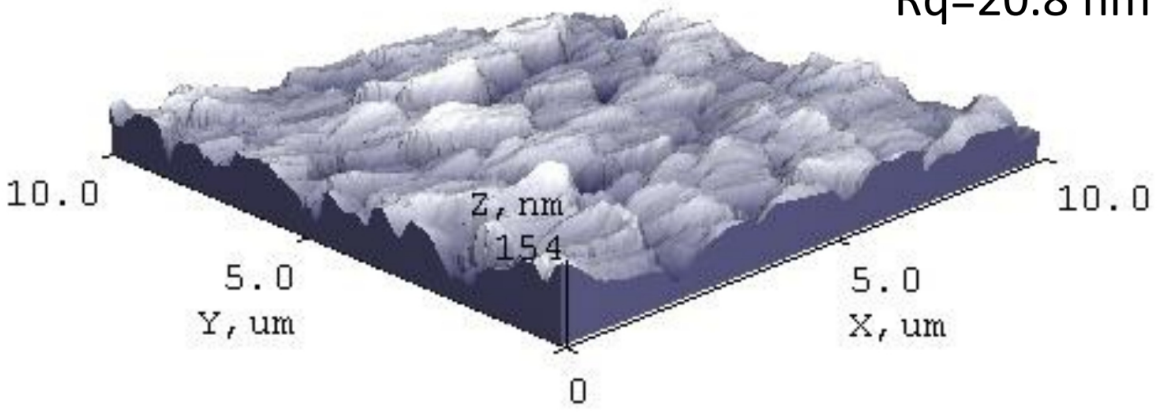

c)

Ra=21.4 nm
Rq=26.2 nm

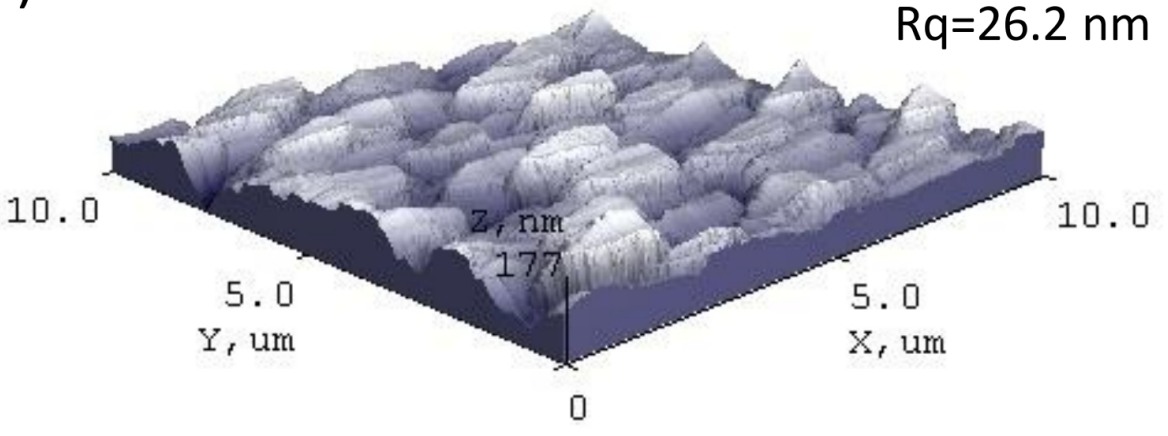

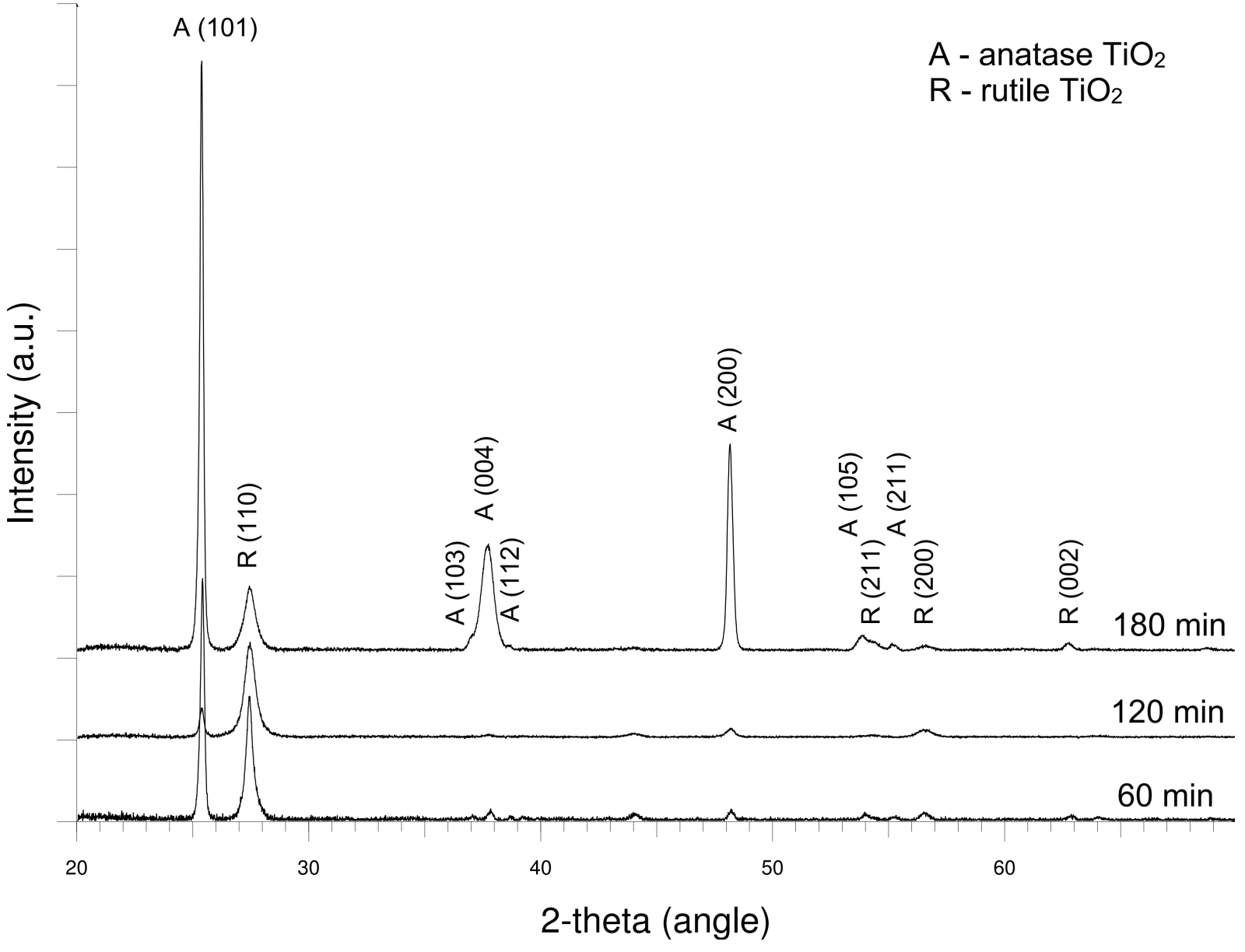
A (101)
A - anatase TiO2
R - rutile TiO2
Intensity (a.u.)
R (110)
A (103)
A (004)
A (112)
A (200)
A (105)
R (211)
A (211)
R (200)
R (002)
180 min
120 min
60 min
20
30
40
50
60
2-theta (angle)

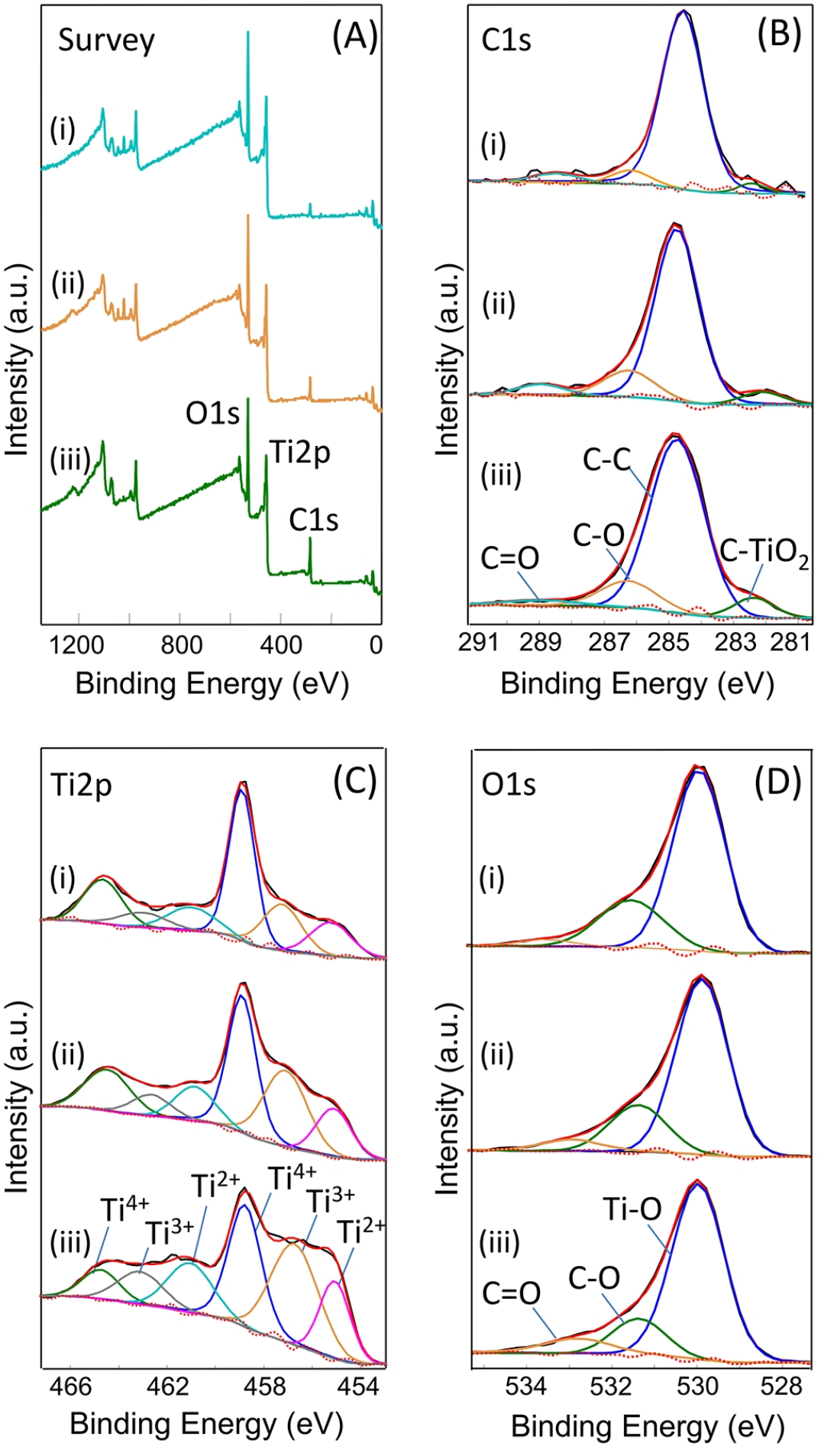
Survey
(A)
(i)
(ii)
(iii)
O1s
Ti2p
C1s
Intensity (a.u.)
1200
800
400
0
Binding Energy (eV)
C1s
(B)
(i)
(ii)
(iii)
C-C
C-O
C=O
C-TiO2
Intensity (a.u.)
291
289
287
285
283
281
Binding Energy (eV)
Ti2p
(C)
(i)
(ii)
(iii)
Ti4+
Ti3+
Ti2+
Ti4+
Ti3+
Ti2+
Intensity (a.u.)
466
462
458
454
Binding Energy (eV)
O1s
(D)
(i)
(ii)
(iii)
Ti-O
C-O
C=O
Intensity (a.u.)
534
532
530
528
Binding Energy (eV)

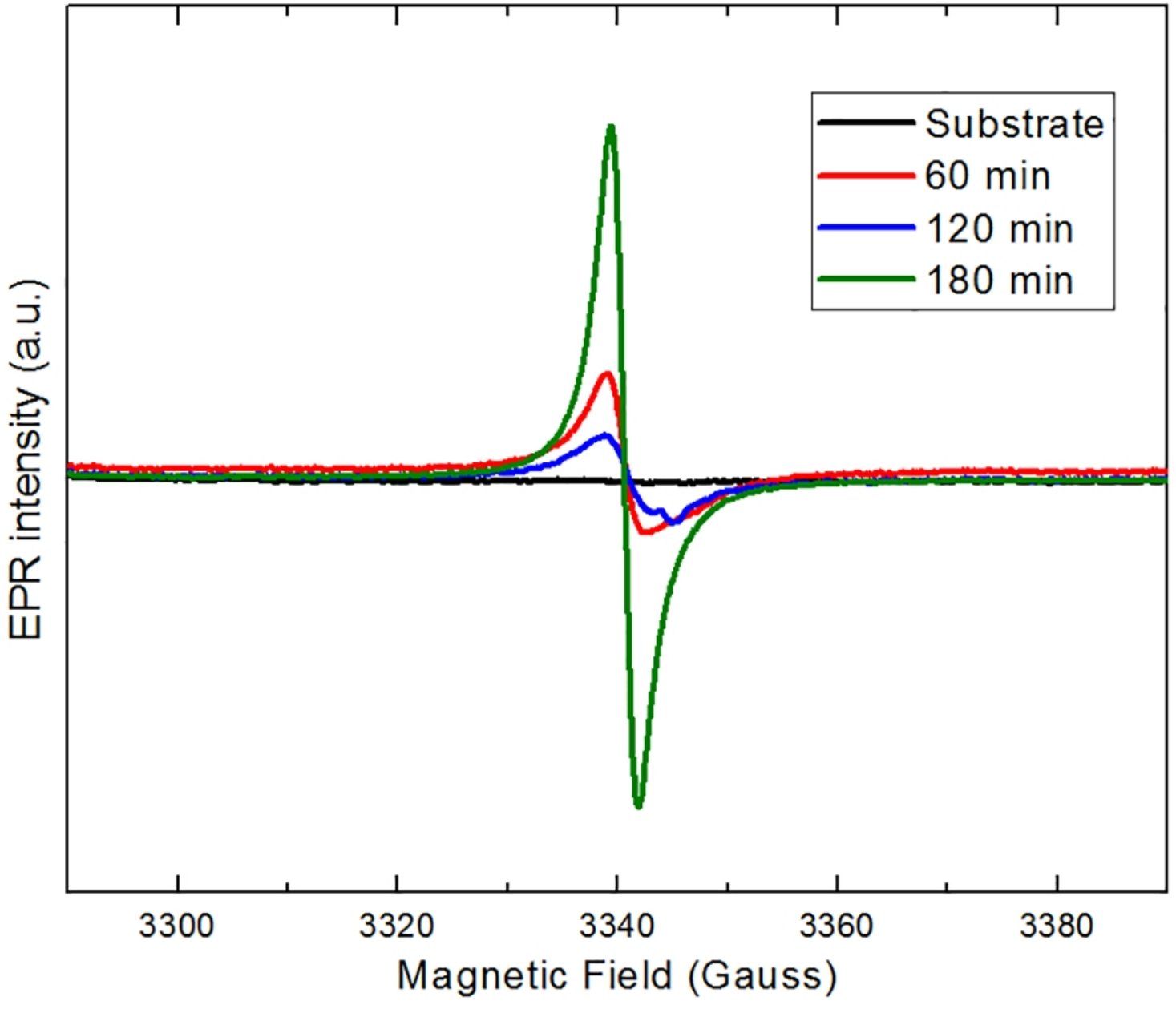
Substrate
60 min
120 min
180 min
EPR intensity (a.u.)
3300
3320
3340
3360
3380
Magnetic Field (Gauss)

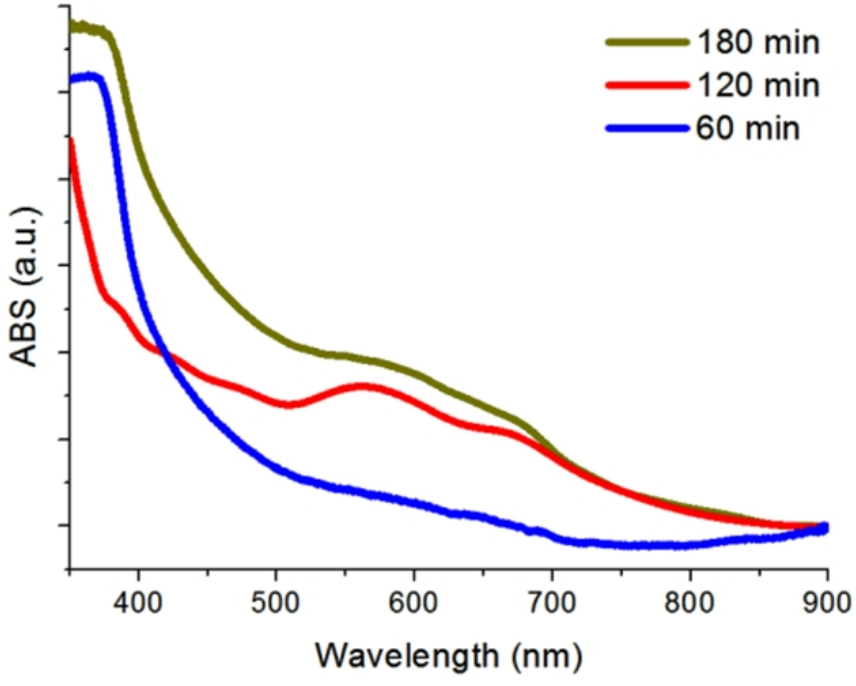
180 min
120 min
60 min
ABS (a.u.)
400
500
600
700
800
900
Wavelength (nm)

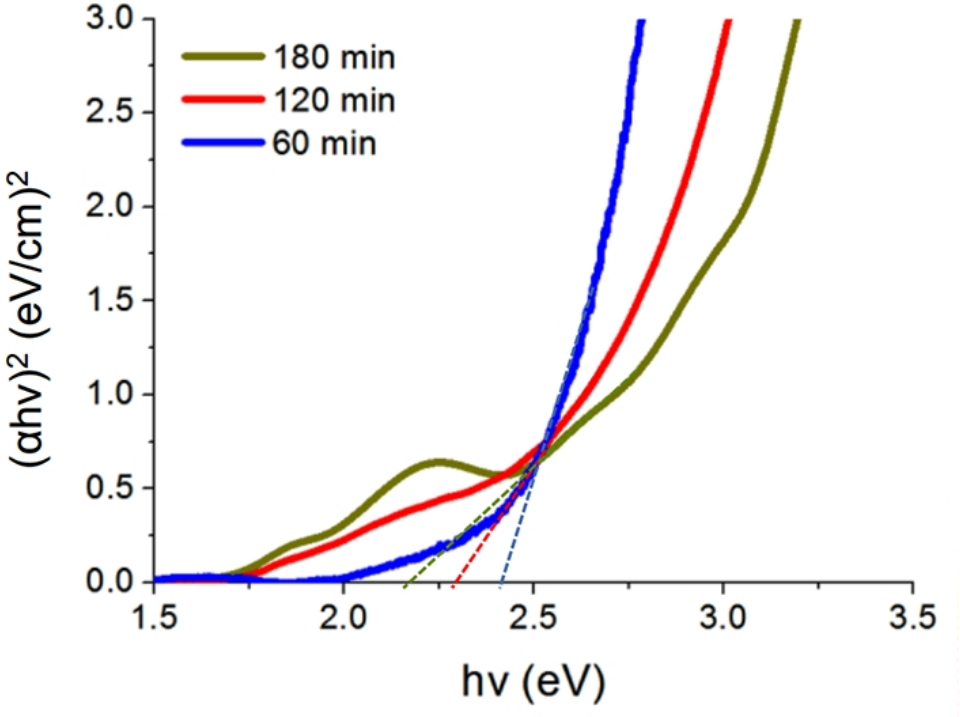
180 min
120 min
60 min
(αhv)² (eV/cm)²
3.0
2.5
2.0
1.5
1.0
0.5
0.0
1.5
2.0
2.5
3.0
3.5
hv (eV)

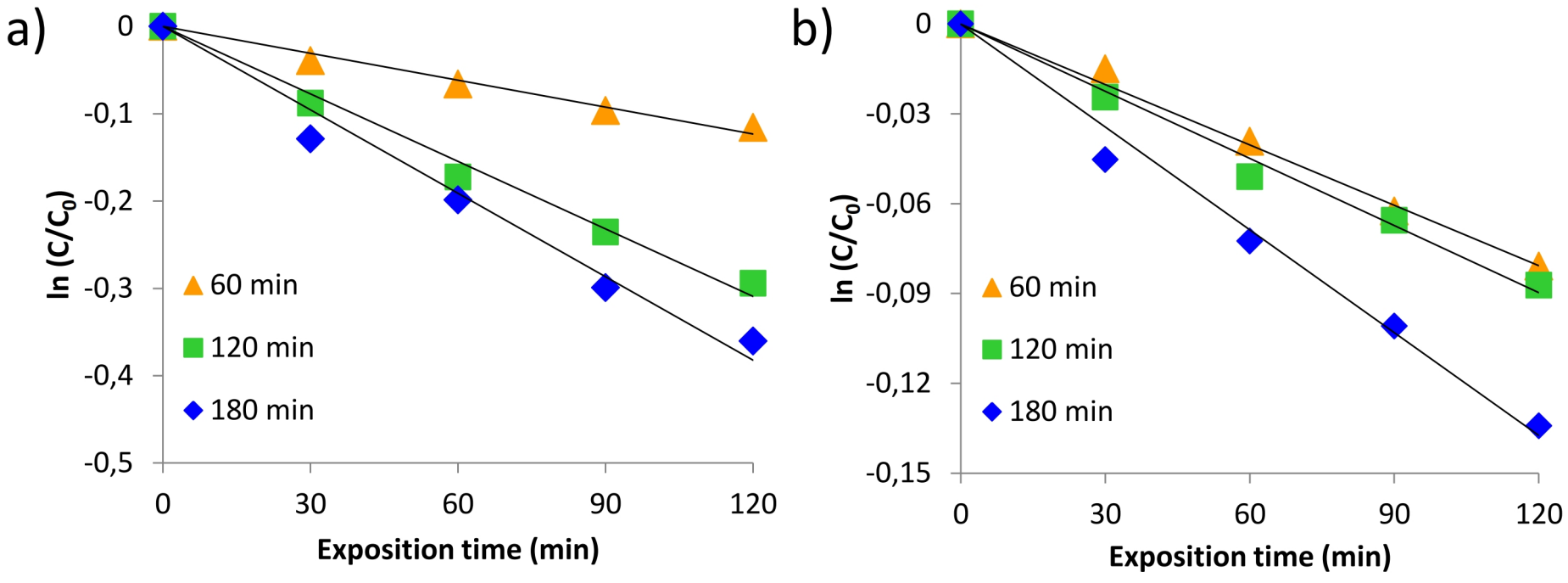
a)
0
-0,1
-0,2
-0,3
-0,4
-0,5
ln (C/C0)
60 min
120 min
180 min
0
30
60
90
120
Exposition time (min)
b)
0
-0,03
-0,06
-0,09
-0,12
-0,15
ln (C/C0)
60 min
120 min
180 min
0
30
60
90
120
Exposition time (min)